

LATE ATOKAN SILICICLASTIC CAVE-FILL DEPOSITS WITHIN PRE-  
ABSAROKAN PALEOKARST IN THE BURLINGTON-KEOKUK LIMESTONE,  
DADE COUNTY, MISSOURI

A Thesis by

Robert W. Turner

Bachelor of Science, Wichita State University, 2009

Submitted to the Department of Earth, Environmental, and Physical Sciences  
and the faculty of the Graduate School of  
Wichita State University  
in partial fulfillment of  
the requirements for the degree of  
Master of Science

December 2011

© Copyright 2011 by Robert W. Turner

All Rights Reserved

LATE ATOKAN SILICICLASTIC CAVE-FILL DEPOSITS WITHIN PRE-  
ABSAROKAN PALEOKARST IN THE BURLINGTON-KEOKUK LIMESTONE,  
DADE COUNTY, MISSOURI

The following faculty members have examined the final copy of this thesis for form and content, and recommend that it be accepted in partial fulfillment of the requirement for the degree of Master of Science, with a major in Earth, Environmental, and Physical Sciences.

---

S.J. Mazzullo, Committee Chair

---

William Parcell, Committee Member

---

Collette Burke, Committee Member

---

D. Paul Rillema, Committee Member

## ACKNOWLEDGMENTS

I would like to thank my advisor, Doc, for the knowledge and guidance he's shown me over the past few years. The experience has been invaluable. Many thanks go to Beau and Brian for the ideas and help in the field. A great debt of gratitude is owed to Cortland Eble for running the paleo samples for this study. I must thank Korban and my father for the help collecting samples and data, and to Jim Puckett and Zach Poland for assisting me with obtaining materials. The KGF and AAPGF funded this research; thanks go to all of the donors whom made this research possible. I would also like to thank the entire faculty in the Geology Department at WSU and my thesis committee for the help, knowledge, and support.

Lastly, gratitude is owed to my parents and family for always being there and assisting me along the way. I am gracious for all the love and support which they have afforded me.

## ABSTRACT

Two siliciclastic-filled paleocaverns within the Mississippian (Osagean) Burlington-Keokuk Limestone, which were formed in pre-Desmoinesian (Middle Pennsylvanian) time, are described from exposures in Dade County, Missouri. Petrographic and sedimentological analyses suggest that these cave-fills were derived from terrestrial sources. The age of the cave-fills were determined to be Late Atokan (Lower Pennsylvanian) based on their spore and pollen assemblage.

One of the caves examined is filled primarily with coarse to fine-grained sand. Sedimentary structures include plane-beds, cross-stratification, scours, flaser bedding, soft-sediment deformed layers, flame structures, and normal-graded bedding. Cave-roof collapse and associated boudinage, as well as slack water shales, separate thick sandstone layers. This paleocavern has been interpreted to have been filled by fluvio-karst processes with sediment entering primarily through sinking streams.

The cave-fill in the other paleocave examined is primarily mudrock, shale, and sandy siltstone with some roof-collapse breccia. These rocks contain abundant organic matter, including wood fragments and charcoal, as well as abundant pyrite and secondary sulfate minerals. This paleocave has been interpreted to have been filled by soil and residuum entering through sinkhole collapses beneath marshes or swamps and by some in-flowing, low-energy water currents.

The recharge points of a cave can be inferred by the type of sediments that it is filled with and recharge points dictate cave geometry. These recharge points can be seen on subsurface maps and an area of possible paleocaves can be drawn between these points. Sandstone cave-fill and fractured limestone host-rock around shale-filled caves are potential hydrocarbon reservoirs in the subsurface of Kansas and northern Oklahoma.

## TABLE OF CONTENTS

Chapter	Page
1. INTRODUCTION .....	1
Introduction.....	1
Study Area .....	2
Purpose.....	3
Methodology.....	10
2. PALEOCAVES AND CAVE-FILL .....	12
Cave-fill Paleontology and Biostratigraphy.....	12
Cave-fill Facies .....	16
Slackwater facies .....	16
Channel facies.....	17
Diamictite facies .....	22
Sediment Provenance.....	22
Diagenesis.....	29
Pyrite formation .....	29
Secondary sulfates .....	30
Secondary porosity.....	31
Cave-System Hydrology and Geometry .....	36
3. Cave-fill in pre-Absaroka caves in the Kansas subsurface.....	39
Pre-Absaroka cave formation in Kansas.....	39
Karst-controlled and cave-fill hydrocarbon reservoirs .....	40
Recognizing cave-fill in bore holes .....	41
Subsurface mapping of paleokarst landscapes.....	43
4. Conclusion .....	48
REFERENCES .....	51
APPENDIXES .....	57
Sandstone mineralogy, grain-size, and texture .....	58
Slackwater grain-size.....	76
Measured porosity and permeability.....	77

## LIST OF FIGURES AND TABLES

Figure	Page
1.1 Road map of the study area.....	3
1.2 Photograph of the western outcrop.....	4
1.3 Photograph of the eastern outcrop.....	5
1.4 Photograph of the southern outcrop.....	6
1.5 Middle Mississippian paleogeography.....	8
1.6 Late Mississippian paleogeography.....	9
1.7 Early Pennsylvanian paleogeography.....	9
1.8 Late Pennsylvanian paleogeography.....	10
2.1 Kansas and Missouri Geological Survey stratigraphic columns.....	14
T2.1 Table of spores and pollen identified within cave-fill.....	15
2.2 Facies relationship of eastern outcrop.....	16
2.3 Slackwater facies (facies A).....	17
2.4 Channel facies (facies B1).....	18
2.5 Channel facies (facies B2).....	19
2.6 Erosional surface in facies B2.....	19
2.7 Channel facies (facies B3).....	20
2.8 Gradational relationship of channel facies, eastern outcrop.....	21
2.9 Diamictite facies (facies C).....	22
2.10 Photomicrograph of an inclusion within a coarse quartz grain.....	24
2.11 Photomicrograph of euhedral bipyramidal quartz.....	24
2.12 Photomicrograph of polycrystalline quartz with large subgrains.....	25

LIST OF FIGURES AND TABLES (continued)

Figure	Page
2.13 Photomicrograph of polycrystalline quartz with many subgrains.....	25
2.14 Photomicrograph of a tripolitic spiculite pebble.....	26
2.15 Late Atokan paleoterrain modified from Rascoe and Adler.....	28
2.16 Late Atokan paleogeography modified from Blakey.....	29
2.17 Selenite gypsum in the slackwater facies.....	30
2.18 Gypsum crust and melanterite alteration.....	31
2.19 Copiapite.....	31
2.20 Photomicrograph of poorly sorted wacke.....	32
2.21 Photomicrograph of facies B1 with abundant matrix content.....	33
2.22 Photomicrograph of carbonate-cemented sandstone.....	33
2.23 Photomicrograph of secondary porosity with corroded grains.....	34
2.24 Photomicrograph of elongated pore from the removal of matrix material.....	35
2.25 Photomicrograph of a moldic pore.....	35
2.26 Cave passage patterns.....	38
3.1 Gamma-ray profile of cave-fill outcrops.....	40
3.2 Suspected cave-fill shown on electric log from sec. 10-32S-22W.....	41
3.3 Suspected cave-fill shown on electric log from sec. 9-30S-22W.....	42
3.4 Cherokee to Mississippian isopach map of northeast Clark County, Kansas.....	44
3.5 Restored Mississippian structure map of northeast Clark County, Kansas.....	45
3.6 Cross-section through a sinking stream in northeast Clark County, Kansas.....	46

# CHAPTER 1

## INTRODUCTION

### **Introduction**

Karst is a landscape shaped by the dissolution of bedrock, typically by meteoric waters on limestone or dolomite, and is characterized by partial or complete subterranean drainage. Karst can be described in terms of time of formation, such as eogenic (formed in loosely- compacted, recently deposited carbonate rocks) or telogenic (formed in well-compacted and indurated carbonates), and in terms of the dissolution responsible for karstification, for example, epigenic (meteoric solutions with atmospheric, soil, and bedrock derived acidity) or hypogenic (rising hydrothermal solutions with H<sub>2</sub>S derived acidity), among others. The broad subject of karst morphology and hydrology are detailed in Jennings (1971), James and Choquette (1985), Jennings (1985), White (1988), Ford and Williams (1989).

Ancient karst landscapes are referred to as paleokarst. Examples of pre-Pennsylvanian paleokarst on the Madison Shelf are given by Sando (1988), on the Leadville Shelf by Evans and Reed (2006), and in the Illinois Basin by Plotnick, et al. (2009). Bretz (1950) estimated that over 1,000 filled paleokarst features were observed by geologists on the western and northern flanks of the Ozark Dome in Missouri. Most of these karst features are sinkholes and enlarged fractures or bedding planes, but several large paleocaves have been described.

Karstification creates sinkholes and caves which act as accommodation space for sediments to be deposited. Cave-fill is a term used to refer to the sediments or rocks which fill paleocaves. Protection of cave-sediments afforded by the cave-roof may allow

for preservation of strata that may otherwise be eroded in surface deposits (Anthony and Granger, 2006) and are comparable to lacustrine deposits in their ability to record continental settings (Sasowsky, 2007). The surrounding limestone host-rock also prevents cave-sediments from severe compaction and may preserve original morphology of macro and micro fossils not seen in other environments (Whiteside and Marshall, 2008; Glasspool et al., 2009).

Cave-fills are also of interest among economic geologists for their potential hydrocarbon reservoirs and ore deposits. Hundreds of filled pre-Pennsylvanian karst features in Missouri were mined for hematite, pyrite, coal, refractory clays, barite, lead, and zinc prior to 1950 (Bretz, 1950). In the subsurface, paleokarst networks and cave-fills influence petroleum reservoirs throughout the world. Loucks (1999), for example, described the characteristics of paleocave carbonate reservoirs and cited examples of such oil fields in the United States and elsewhere.

### **Study Area**

Two paleocaves, and several other small associated karst features, have recently been exposed along state highway 39 in Dade County, Missouri (Fig. 1.1). The northern paleocave is exposed in axial cross-section on the east and west sides of the highway and is filled mostly with sandstone. The western exposure (Fig. 1.2) is 20 m wide and is obscured by a spring as well as plant growth. The northern side of the original cave passage was also destroyed by post-depositional collapse. The eastern exposure (Fig. 1.3) is 30 m wide, and its stratification and morphology are well preserved, although it also displays post-depositional collapse. Both exposures are 7 m tall, but their bases are not exposed. Hence, the caves are larger than what is exposed in these roadcuts. The

Burlington-Keokuk Limestone beds in which the caves are present dip to the south on the northern end of the exposures, and they are nearly flat on the southern end. There is also a fracture evident in the cave-roof on the eastern cave, and its southern wall is nearly vertical. Together, these features suggest the cave passage developed along high angle fractures as discussed, for example, by (White, 1988).

The southern paleocave (Fig. 1.4) is exposed in lateral cross-section on the east side of the highway, and it is filled mostly with dark gray to black mudrock and shale. The cave-fill exposure is 90 m long and 3-5 m high. This passage dips to the south and cuts across beds of the Burlington-Keokuk, suggesting that this passage formed along a low angle fracture since no bedding plane control is evident.



Figure 1.1. Road map and relief map of the study area. The cave-fills were exposed by construction of a new section of highway bypassing the town of South Greenfield, Missouri. Maps from [www.randmcnally.com](http://www.randmcnally.com) accessed April, 2010.

## Purpose

The purposes of this study are: 1) describe the exposed 2-D geometry of the paleocave passages and propose a likely 3-D morphology of the cave-system; 2) describe the sedimentary features of the cave-fill and determine their depositional environment as well as their environmental implications; and 3) develop a model for predicting sandstone filled paleocaves in the subsurface of Kansas that may be economic petroleum reservoirs.

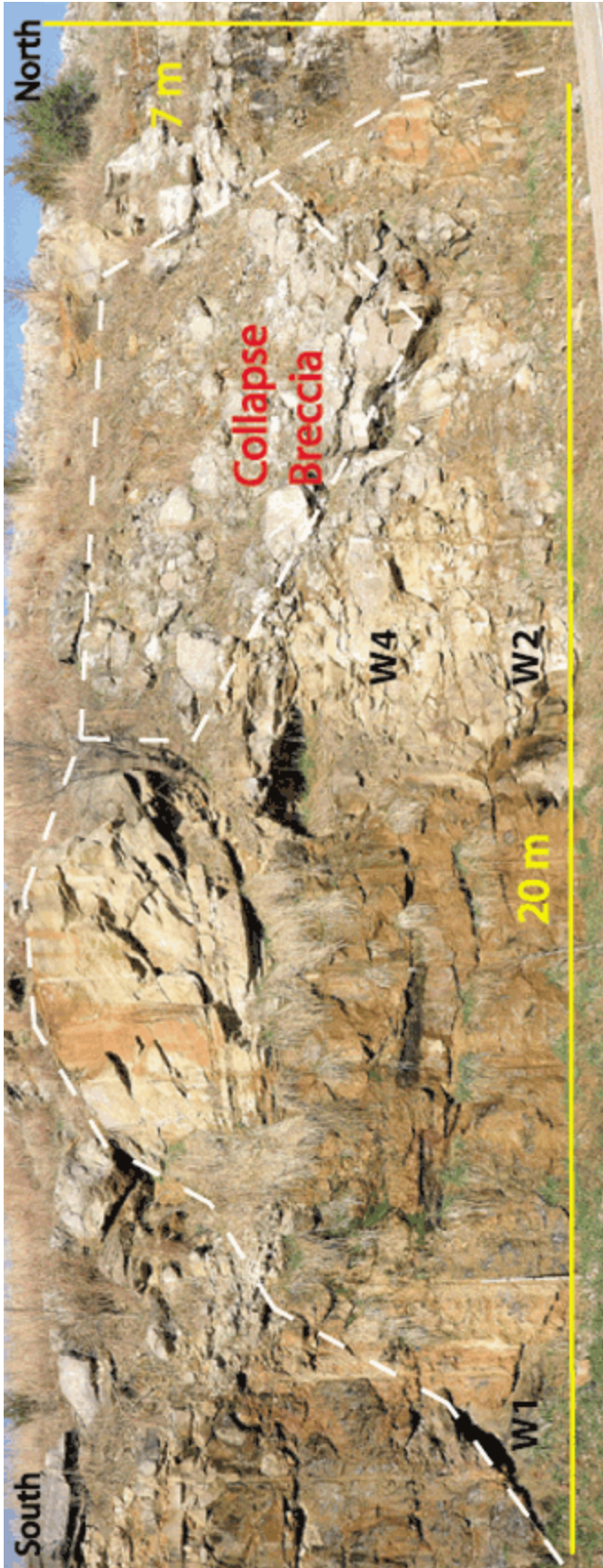


Figure 1.2. Northern cave-fill, west side. This cave-fill is obscured by an active spring, plant growth, and by cave-roof collapse on the north end. The collapse of the roof is post depositional but prelithification. The differences between this outcrop and the outcrop across the road of the same paleocave are indicative of the heterogeneity within cave passages.



Figure 1.3. Northern cave-fill, east side. A large portion of this cave-fill is porous sandstone. The collapse breccia occurred after deposition, but before lithification, creating boudinage structures. The cave-roof is highly fractured on the north end due to compaction of the finer sediments on that end of the fill.



Figure 1.4. Southern cave-fill. The smell of  $H_2S$  gas is strong at this outcrop and the limestone around the cave-fill is highly weathered, sometimes called “rauwanke” in Europe. The limestone exposure in the ditch below the cave-fill appears polished. Portions of the cave-roof are highly fractured.

## **Geographic Setting**

The siliciclastic-filled paleocaves near South Greenfield are in the Osagean (Middle Mississippian) Burlington-Keokuk Limestone. The area was situated on the western flank of the Ozark Dome, at approximately 10 degrees south latitude at this time (Gutschick and Sandberg, 1983). The Ozark Dome was bordered by the Forest City Basin to the north and west and by the Illinois basin to the east. The Burlington-Keokuk Limestone in southwest Missouri is a thick-bedded, coarse crinoidal grainstone that was deposited on a regionally extensive shallow carbonate shelf. White, vitreous, and nodular or layered chert is common throughout the formation. In the area of this study, the Burlington-Keokuk is unconformably overlain by Meramecian (Middle Mississippian) or Middle Pennsylvanian rocks, however no upper contact with such rocks is exposed at the outcrops studied. The Burlington-Keokuk was lithified by meteoric waters (Kaufman, et al., 1988), probably during subaerial exposure after deposition.

The Burlington-Keokuk Shelf was subaerially exposed during a eustatic sea level fall around 330 Ma. (Saunders and Ramsbottom, 1986) corresponding to Gondwana glaciation (Veevers and Powell, 1987) in the Late Mississippian. This exposure surface represents the boundary between the Kaskaskia and Absaroka Sequences (Sloss, 1963). Tectonic movement from the collision between Laurussia and Gondwana influenced the deposition and structure of Mississippian strata beginning in Kinderhookian (Early Mississippian) time (Mazzullo et al., 2011) and continued into the Pennsylvanian. Fractures and faults as a result of this tectonism acted as conduits for the channeling of meteoric water where subsequent limestone dissolution and fracture enlargement occurred. This long period of karstification on the Burlington-Keokuk Shelf continued

until transgression periodically submerged the mid-continent during the Middle Pennsylvanian (Heckel, 1986). Paleogeographic maps of this time period are shown in Figures 1.5 to 1.8.

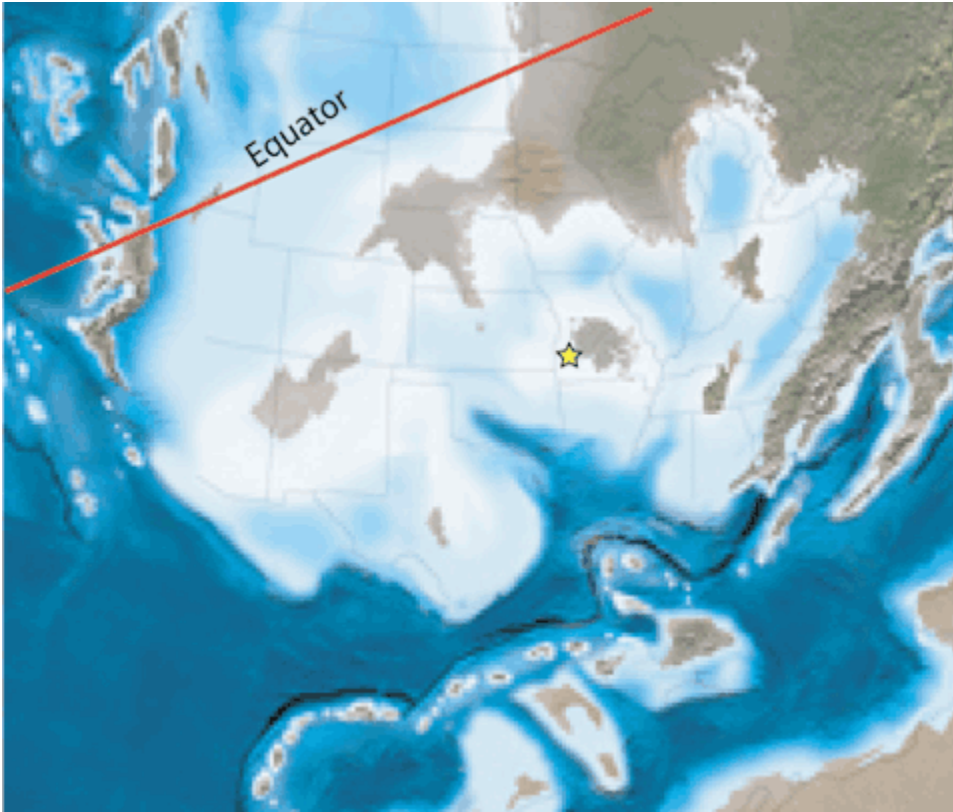


Figure 1.5. Middle Mississippian; maximum Kaskaskian transgression. Paleogeography during Burlington-Keokuk deposition. Tectonic affects from the Laurussia-Gondwana collision are already influencing Mississippian deposition by this time. The yellow star marks the study area. Modified from Blakey (2003).



Figure 1.6. Late Mississippian; Eustatic sea level drop. The yellow star marks the study area. Modified from Blakey (2003).



Figure 1.7. Early Pennsylvanian; sea level began to rise, continued karstification on the Burlington-Keokuk Shelf. Ouachitas were a major sediment source in the Arkoma Basin. The yellow star marks the study area. Modified from Blakey (2003).



Figure 1.8. Late Pennsylvanian; pre-Pennsylvanian karstification ceases on the entire Burlington-Keokuk Shelf as it is submerged by a shallow sea. The yellow star marks the study area. Modified from Blakey (2003).

## Methodology

Each outcrop was measured in detail and photographed. Samples were collected from each cave-fill; samples that were analyzed in detail are marked on the outcrop photographs. Thin-sections were made from 15 select sandstone samples for petrographic analysis. Grain-size, roundness, and mineralogy were recorded for 100 grains on each slide at 80X magnification. These data were entered into Excel and grain-size statistical parameters (mean grain-size, sorting, and skewness) were calculated using graphical methods from Folk and Ward (1957). Porosity and matrix material was also measured in thin-section. Porosity and permeability of six sandstone plugs were measured by Weatherford Laboratories of Houston. This data was used for reference in estimating porosity in the thin-sectioned samples. Five sandy shale and mudrock samples

were weighed, disaggregated in water, and then dried. The samples were then dry-sieved to determine the weight percentage of clays, silts, and sand. A Rigaku Miniflex II X-Ray diffractometer was used to determine the mineralogy of the non-sand portion of the cave-fill.

Four carbonaceous shale samples were sent to the Kentucky Geological Survey for palynological analysis by Cortland Eble. The samples were macerated in water and placed in HF for dissolution of silica minerals. Spore and pollen assemblages were observed and identified for biostratigraphic correlation of the cave-fills. Detailed quantitative analysis of the palynologic assemblages was not conducted, therefore environmental interpretations using these data are uncertain.

A hand-held gamma-ray spectrometer was used to measure natural radioactivity on two of the outcrops. Measurements were taken vertically on 0.5 meter spacing starting and ending on the limestone host-rock. The measurements were then converted to API units and plotted on a graph identical to the scale used for subsurface electric well-logs. Two paleogeographic maps of the paleokarstic Mississippian landscape were prepared using the GIS mapping software GeoGraphix. An isopach (thickness) and paleotopographic map were used to depict karst on the Mississippian subcrop and show karst-control on hydrocarbon reservoirs. Formation tops were checked for accuracy and well bores that encountered suspected cave-fills were plotted on the maps. Wells that penetrated the base of the Mississippian are scarce in the study area, therefore a grid-to-grid operation was used with the Stotler Formation to create this map, a technique used, for example, by Sando (1988).

## Chapter 2

### PALEOCAVES AND CAVE-FILL

#### Cave-fill Paleontology and Biostratigraphy

Four samples (S1B and S1T from the southern cave-fill, and EM and ET from the northern cave-fill) were used for palynological identifications. Sample EM did not contain a sufficient yield for a meaningful analysis. The other three samples contained a high yield of well-preserved palynomorphs which are detailed in Table 2.1. Among the samples were spores and pollen from *Torispora securis*, *Triquitrites sculptilis*, *Dictyotriletes bireticulatus*, *Endosporites globiformis*, *Laevigatosporites globosus*, and *L. desmoinesis* which indicate a Late Atokan age. The gymnosperms *Torispora securis* and *Triquitrites sculptilis* did not become abundant until Late Atokan time and *Dictyotriletes bireticulatus* becomes extinct towards the end of the Late Atokan (Peppers and Brandy, 2007).

Ferns, especially tree ferns, did not become abundant until the Middle Atokan and remained abundant until the Early Desmoinesian (Peppers and Brandy, 2007). A relative abundance of fern species suggests a seasonally drier climate as has also been documented in the Illinois Basin (Peppers, 1996) and Appalachian Basin (Phillips et al., 1985) during this same time period. The cave-fill also contains charcoaled wood fragments which is further evidence of at least a periodically drier climate during the Late Atokan relative to the rest of Pennsylvanian Period.

Correlating Atokan and Lower Desmoinesian strata in southwest Missouri, eastern Kansas, and northeast Oklahoma has proven difficult for stratigraphers because of the lateral discontinuity and diachronous nature of many of these rocks (Ebanks, 1979).

A clear discrepancy exists between the Kansas and Missouri geological surveys for the placement of the Atokan and Desmoinesian boundary (Fig. 2.1). Peppers and Brandy (2007), for example, found the Riverton Formation to be Lower Desmoinesian in the Forest City Basin based on palynological correlation and placed the boundary below this marker bed. Peppers and Brandy (2007) also included the Atokan aged rocks in the Forest City Basin in the Cherokee Group because of the lack of formal nomenclature associated with these strata. The cave-fill in the northern cave is not equivalent to any formally named unit by either state survey. The cave-fill in the southern cave is considered to be Riverton Formation by the Missouri Geological Survey.



Table 2.1

<u>Spore Taxa/Affinity</u>				<u>Spore Taxa/Affinity</u>			
	S1B	S1T	ET		S1B	S1T	ET
Lycospora pellucida	X	X	X	<b>Total Tree Ferns cont.</b>			
L. pusilla	X	X	X	Knoxisporites rotatus	X		
L. granulata	X	X		K. tiradiatus	X		
L. orbicula	X			Reticulitriteles clatriformis			
L. micropapillata	X						
Crassispora kosankei	X	X	X	Reticulitriteles reticulocingulum	X		
<b>Total Lycopsid Trees</b>				Punctatisporites planus	X		
				P. nahannensis			
Densosporites annulatus	X			P. aerarius	X		
D. triangularis				P. pseudolevatus	X	X	
D. sphaerotriangularis	X		X	P. stramineus	X		
D. intermedius	X		X				
D. lobatus				Verrucosisporites verrucosus	X	X	
D. spinosus	X		X	V. donarii	X		
Radiizonates difformis - rotatus		X		<b>Total Small Ferns</b>			
Cingulizonates loricated		X		Calamospora breviradiata	X	X	
				C. pedata		X	
Endosporites globiformis	X	X		C. microrugosa	X	X	
E. pallidus	X	X					
E. micromainifestus	X	X		Laevigatosporites minor	X	X	X
				L. desmoinensis	X	X	X
Anacanthotriteles spinosus	X			L. vulgaris		X	
<b>Total Small Lycopside</b>				Reticulatisporites muricatus	X		
Punctatisporites minutus	X	X	X	<b>Total Calamites</b>			
				Florinites florini	X		
Laevigatosporites globosus	X	X		F. mediapudens	X	X	X
L. minimus	X	X		F. milloti	X	X	
Torispora securis	X	X		Vesicaspora wilsonii	X		
<b>Total Tree Ferns</b>				Pityosporites westphalensis	X		
Granulatisporites piroformis	X	X	X	<b>Total Gymnosperms</b>			
G. adnatoides	X	X					
G. granulatus	X	X	X	Triquitrites bransonii	X	X	X
G. tuberculatus	X			T. minutus		X	
				T. trimarginatus	X		
Cyclogranisporites minutus		X		T. subspinosus			
				T. sculptilis	X	X	
Lophotriteles microsaetosus	X	X	X				
L. commissuralis	X	X		Trochospora mastospinosa	X		
L. insignitus	X						
				Anaplanisporites baccatus	X		
Leiotriteles subadnatoides	X	X	X				
L. adnatus	X	X		Stenozonotriteles lycosporoides	X		
L. priddyi				S. bracteolus	X	X	
L. sphaerotriangulus		X		S. coronatus		X	
L. inflatus	X						
L. levis	X	X		Dictyotriteles bireticulatus	X		
Acanthotritele triquetrus	X			Echinatispora spinosa	X		
A. aculeolatus	X						
				Zosterosporites triangularis	X		

## Cave-fill Facies

The cave-fills are divided into three lithofacies: the slackwater, channel, and diamictite facies. The facies relationship of the eastern outcrop, which is the most complex, is shown in Figure 2.2. The channel facies is further divided into three subfacies based on texture. The same facies of modern fluviokarst sediments described by Bosch and White (2004) are also present in this study area. The channel lag is the only facies not found in the paleocaves but likely occurs in the unexposed base of the north cave-fill. Soft-sediment deformed layers occur in all facies and dewatering structures are present in the finer grained facies of the cave-fill.

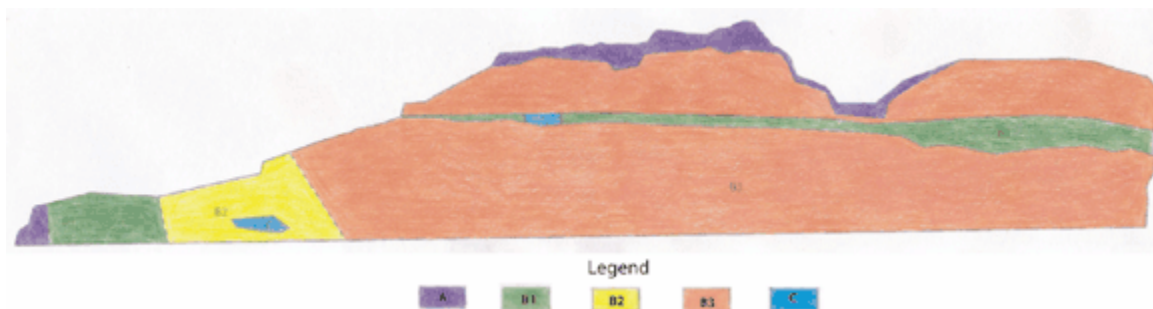


Figure 2.2. The facies relationship in the northern cave-fill, eastern side. The channel facies comprises all of the cave-fill in this section except for slackwater facies on the northern end and capping the fill, as well as minor diamictite deposits.

### *Slackwater facies*

The slackwater facies (facies A, Fig. 2.3) consists of gray to black carbonaceous sandy and silty quartz mudrock and shale. The sand sized portion is clear quartz, detrital chert, plant fragments, charcoal, pyrite nodules, and what appear to be reworked rounded mud clasts. My interpretation is that most of the sediment in this facies was carried as suspended load and deposited during the backflow that occurred during flooding. Sediment entered the cave-system via runoff into sinkholes, diffuse infiltration of soil and regolith through open fractures and enlarged joints in the limestone, from insoluble

residues of the surrounding limestone, and from sediments carried backwards into the cave-system from the discharge point during flooding of the surface stream. The Burlington-Keokuk Limestone was found to contain 4.4% insoluble residues that included quartz, chert, pyrite, and glauconite. Insoluble residues commonly line cave-walls and roof in modern caves and was preserved in portions of the paleocaves in this study. Facies A comprises the bulk of the south cave-fill.



Figure 2.3. An example of the slackwater facies. The arrow points to a piece of charcoal.

### *Channel facies*

The channel facies comprises the bulk of the northern cave-fill and is divided into three subfacies (B1, B2, and B3). Facies B1 (Fig. 2.4) is a flaser, wavy, and lenticular bedded very fine grained lithic sandstone. This type of bedding has traditionally been

used to infer a tide dominated depositional environment but this sedimentary structure is also a common occurrence in perennial and ephemeral fluvial sediments (Bhattacharya, 1997; Martin, 2000). To the author's knowledge, bedding of this type has never been described in cave sediments. This facies is found at the base of the southern end on the west outcrop, on the northern side of the eastern outcrop, and in lenses within the southern cave-fill. The very fine sand ripples and mud drapes are inferred to have been deposited under fluctuating low and stagnant hydraulic currents respectively.



Figure 2.4. Facies B1, lenticular bedded silty very fine sandstone. Sample W1.

Facies B2 (Fig 2.5) is a moderately sorted very fine grained lithic arenite. Some of the layers contain shale wisps and mud chips but differs from facies B1 that it lacks

mud drapes and significant matrix material. Erosional surfaces (Fig 2.6) indicate turbid flow, a feature not seen in facies B1. This facies is located on the northern end of the eastern outcrop.



Figure 2.5. Facies B2, This sample is moderately well sorted with minor amounts of matrix material and shale wisps.



Figure 2.6. Erosional surface in facies B2. Pen for scale.

Facies B3 (Fig 2.7) is a moderate to poorly sorted fine to very coarse grained sandstone. The sandstones include lithic arenites and wackes. Common sedimentary structures include low angle planar cross-bedding, trough cross-bedding, scours, and ripples. Individual beds were typically thick-bedded and normal graded. Deposition of facies B3 is inferred to have taken place during the waning stages of floods. Erosional surfaces indicate the entrainment stage of these high flow events when turbidity was highest. This erosional surface is generally overlain by a poorly sorted very coarse grained section that fines upward into laminar bimodal coarse and medium-grained sand that then fines into a medium to fine grained moderately well sorted sand. Mud drapes were either eroded by the following flood event or hydraulic conditions were never stagnant in this portion of the fill to have allowed for subsequent deposition of mud.



Figure 2.7. Facies B3, this sample has low-angle planar cross-bedding and plane beds.

The sediment that comprises the channel facies is inferred to have entered the cave-system via a sinking stream. A mixed fluvial-tidal system can not be ruled out, but unidirectional dip directions of cross-stratification to the west as well as the lack of herringbone cross-stratification and tidal rhythmites suggest tidal influence on deposition, if any, was overwhelmed by fluvial processes (Gastaldo, 1995).

Most sediment transport in modern caves takes place during floods and is deposited during the waning stages of flow (Bosch and White, 2004). This is the interpreted depositional model for the channel facies in these paleocaves. Passage geometry seemingly affected flow velocity shown by the decrease in flow energy towards the north on the eastern outcrop where the channel subfacies exhibit a gradational relationship (Fig. 2.8). The cave-roof is lower in this portion of the cave passage and apparently restricted flow to the extent that the laminar residuum lining the cave-wall was never eroded.

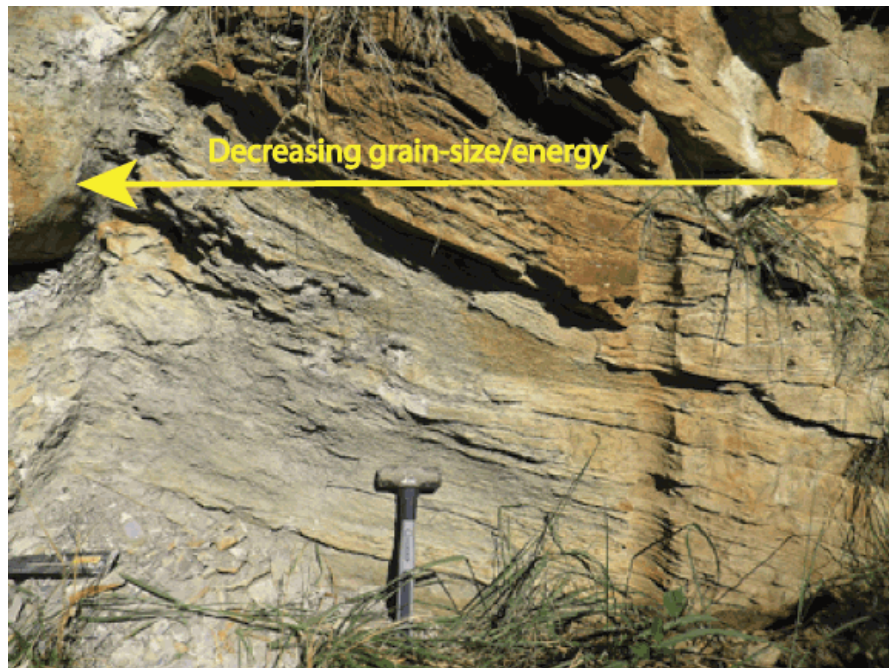


Figure 2.8. The northern end of the eastern outcrop. Facies B1 on the left is shown grading into facies B2 towards the right. Hammer for scale.

### *Diamictite facies*

The diamictite facies (facies C) is an unsorted mass flow deposit consisting of chert and limestone pebble to boulder sized clasts in a sandy mud matrix (Fig 2.9). This facies was deposited as a result of sudden sinkhole collapses and as a mud and gravel slurry during floods. The best example of this facies is on the northern end of the east outcrop. The diamictite here is preserved on account of the retarded current in this portion of the paleocave.

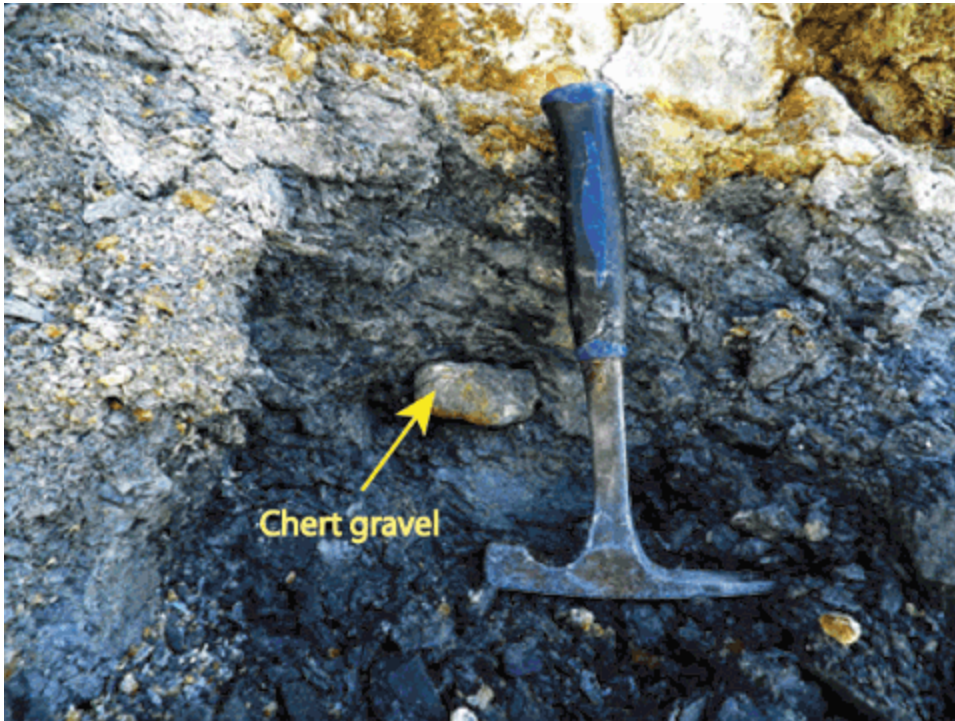


Figure 2.9. Facies C, diamictite. Hammer for scale.

### **Sediment Provenance**

Sandstone petrography and previous work on the Late Atokan paleogeography was used to determine the provenance of the cave-fill. A detailed review on determining the provenance of sandstones is given by Blatt et al. (1980). A wide range of grain roundness from well rounded to very angular were observed, but most grains were

subangular. Mean grain size ranged from very fine sand in sample W1, fine sand in samples EE2 and EE3, and coarse sand in samples W2 and E3. The other ten samples had a mean grain size of medium sand. Quartz grains with inclusions (Fig. 2.10) and composite (polycrystalline) quartz grains were common in the samples and suggest a first-cycle origin with sediments undergoing limited exposure in the sedimentary environment (Blatt, 1967). Quartz overgrowths were common in some samples and rare in others. In several samples, sample E17 for example, quartz overgrowths were observed sporadically throughout the sample and may suggest a polycyclic origin. Together, these data suggest a diverse source area with several provenances for the sandstone cave-fill.

Quartz grains comprised 81-96% of the samples examined. These quartz grains exhibited a range of extinctions under cross-polar light that ranged from straight extinction to very highly undulose, suggesting sources from igneous and metamorphic rocks. Coarse-grained straight extinction quartz is most likely to have come from a plutonic igneous source (Blatt, et al., 1980). Some euhedral bipyramidal quartz grains (Fig. 2.11) with straight extinction were also observed. These grains may indicate a volcanic source area.

Lithic fragments comprised 4-18% of the samples examined. Polycrystalline quartz grains (Fig. 2.12)(Fig. 2.13) were considered lithic fragments in this study and were the most common lithic grain counted. Polycrystalline quartz grains with sutured contacts are additional evidence of a metamorphic source area. Detrital chert grains were also common in the samples and were derived from sedimentary sources. One of these chert grains in sample E7 was derived from a spiculite (Fig. 2.14). Shale clasts were also

observed among the lithic portion of the sandstones. Feldspars were uncommon within the samples, consisting of less than 4% of the grains counted.

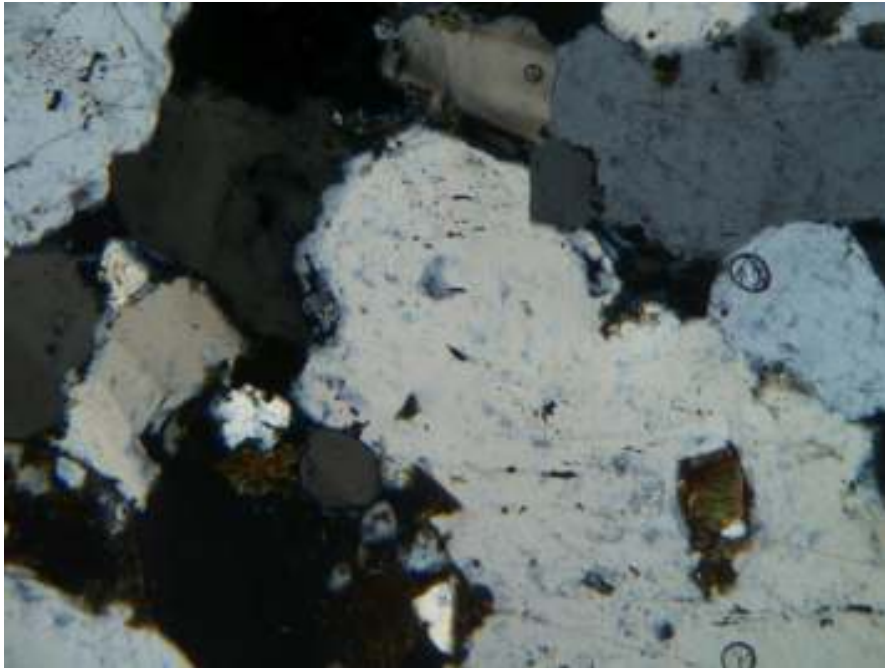


Figure 2.10. Sample E3. A coarse-grained monocrystalline quartz grain with a biotite inclusion (bottom right). Quartz grains with inclusions are less stable than grains without inclusions and are evidence of a first-cycle sediment. 80X magnification.

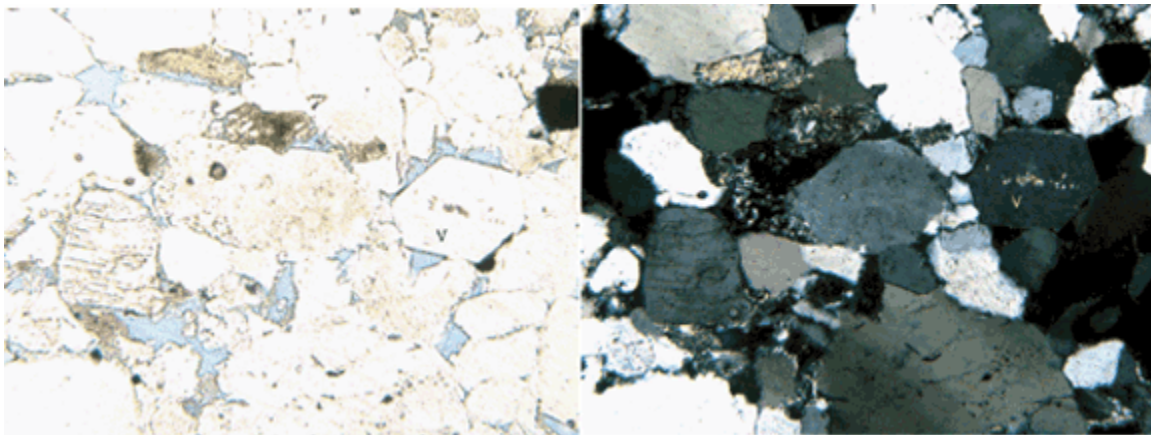


Figure 2.11. Sample E17. A euhedral bipyramidal quartz grain (V) indicative of a volcanic source. 80X magnification.

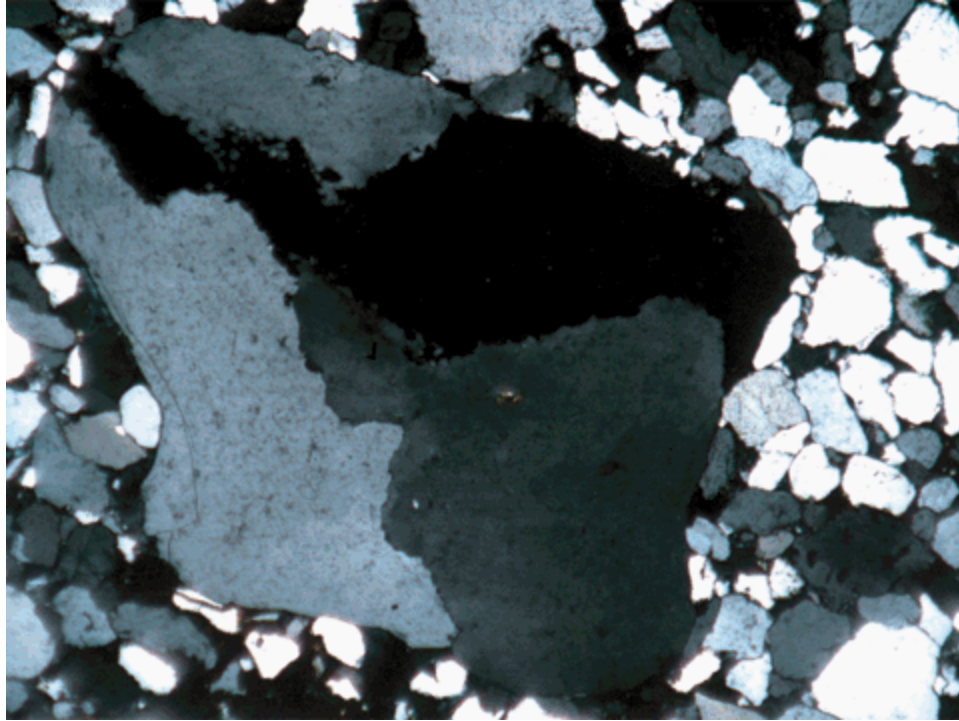


Figure 2.12. Sample E11. A polycrystalline quartz pebble with sutured contacts at 20X magnification. This is likely from a metamorphosed phaneritic igneous rock.

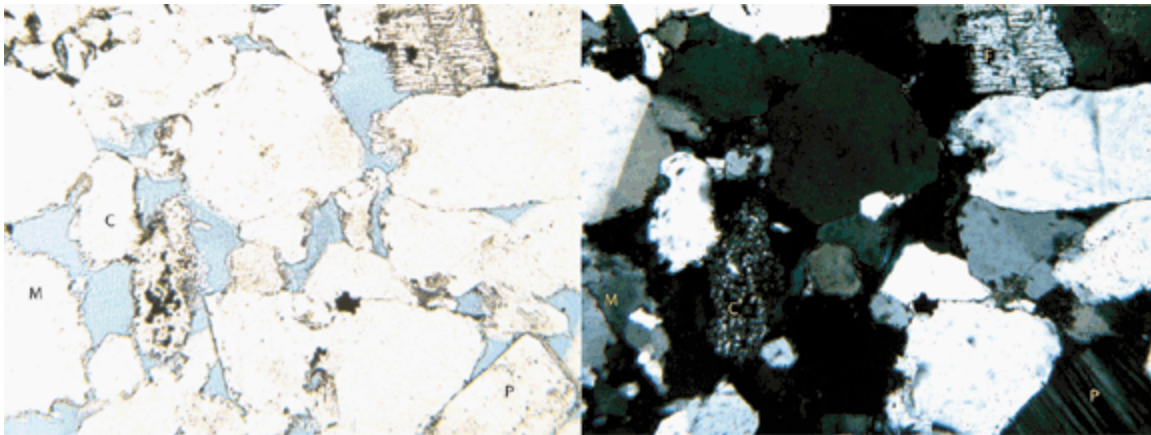


Figure 2.13. Sample E12. A polycrystalline quartz grain (M), these grains are from a metamorphic source rock. Also pictured in this slide is a subangular plagioclase grain with polysynthetic twinning (P) and a chert grain (C). 80X magnification.

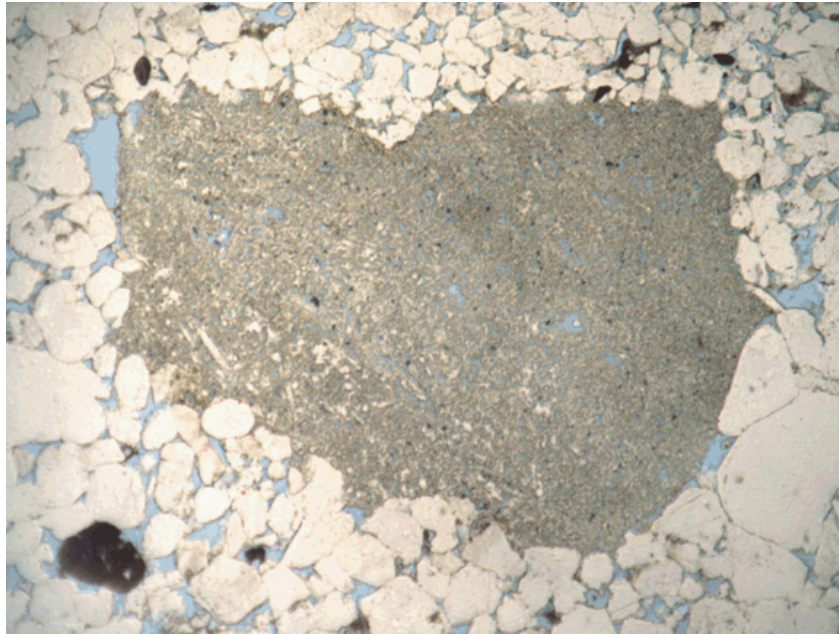


Figure 2.14. Sample E7. A tripolitic spiculite pebble at 20X magnification.

Several igneous and metamorphic source areas existed in the mid-continent during the Late Atokan. These areas included the Canadian Shield to the north, Nemaha Ridge to the west, Ouachita Mountains to the south, and Ozark Dome to the east of the study area. The Illinois and Forest City Basins to the north of the study area were depositional centers during the Atokan through Desmoinesian with up to 755 feet of these deposits (Howes, 1988) and would have made any source of clastics from the Canadian Shield unlikely. The Forest City Basin was also the depositional center for sediments shed from the Nemaha Ridge during the Late Atokan. Wanless, et al. (1970) describe deltas of this age prograding into the Forest City Basin from the west and north which represent deposition from these source areas. This leaves the Ouachita Mountains and Ozark Dome as possible sources of sediment for the cave-fill.

The Ouachita Mountains were rapidly uplifted from the collision between Gondwana and Laurussia during the Atokan. This event also created the Arkoma Basin

to the north of the Ouachitas. Rapid uplift of the Ouachitas and down-warping of the Arkoma Basin resulted in over 10,000 feet of Atokan-aged rocks in the Arkoma Basin which was briefly filled in during the Late Atokan (Rascoe and Adler, 1983). Sediments continued to be carried north by streams after the basin was filled, where they were eventually deposited in the paleocaves. Westward and northwestward progradation of early to mid-Pennsylvanian sediments in the study area were also discussed by Wanless, et al. (1970), suggesting a southern and eastern source for the sediment. Crystalline rocks were also exposed on the southeast Ozark Dome in the St. Francis Mountains during the Late Atokan but these rocks are nearly all unmetamorphosed extrusive igneous rocks (Kisvarsanyi, 1974). The Ozark Dome therefore was not the source of the metamorphic quartz grains in the cave-fill and were likely only a minor source of sediment on account of its low positive relief (Rascoe and Adler, 1983). The Ouachita Mountains, which was a high relief area during the Late Atokan, therefore may have provided most of the sand in the cave-fills.

The detrital spiculitic tripolite pebble (see Fig. 2.14) is also evidence of an overall southern source. Major local sources of detrital chert during the Late Atokan include the Osagean Burlington-Keokuk Limestone and Reed Springs Formation, both of which are not spiculitic in the outcrop area of Missouri, Arkansas, and Oklahoma (Mazzullo et al., 2011). Spiculitic chert is present, however, to the west in the Cowley facies of the Reed Springs Formation in southern Kansas and northern Oklahoma (Mazzullo et al., 2009). This grain may have come from the Cherokee Platform to the southwest, a low relief positive area during the Atokan (Rascoe and Adler, 1983). Reworked Chesterian pollen and spores, including *Endosporites pallidus*, *E. micromanifestus*, *Stenozonotriletes*

*bracteolus*, *S. coronatus* and *Trochospora mastospinosa*, also suggest erosion off the Hindsville and Batesville Formations which were deposited on the Cherokee Platform. Late Atokan paleogeographic maps, revised to reflect this data, are shown in Figures 2.15 and 2.16.

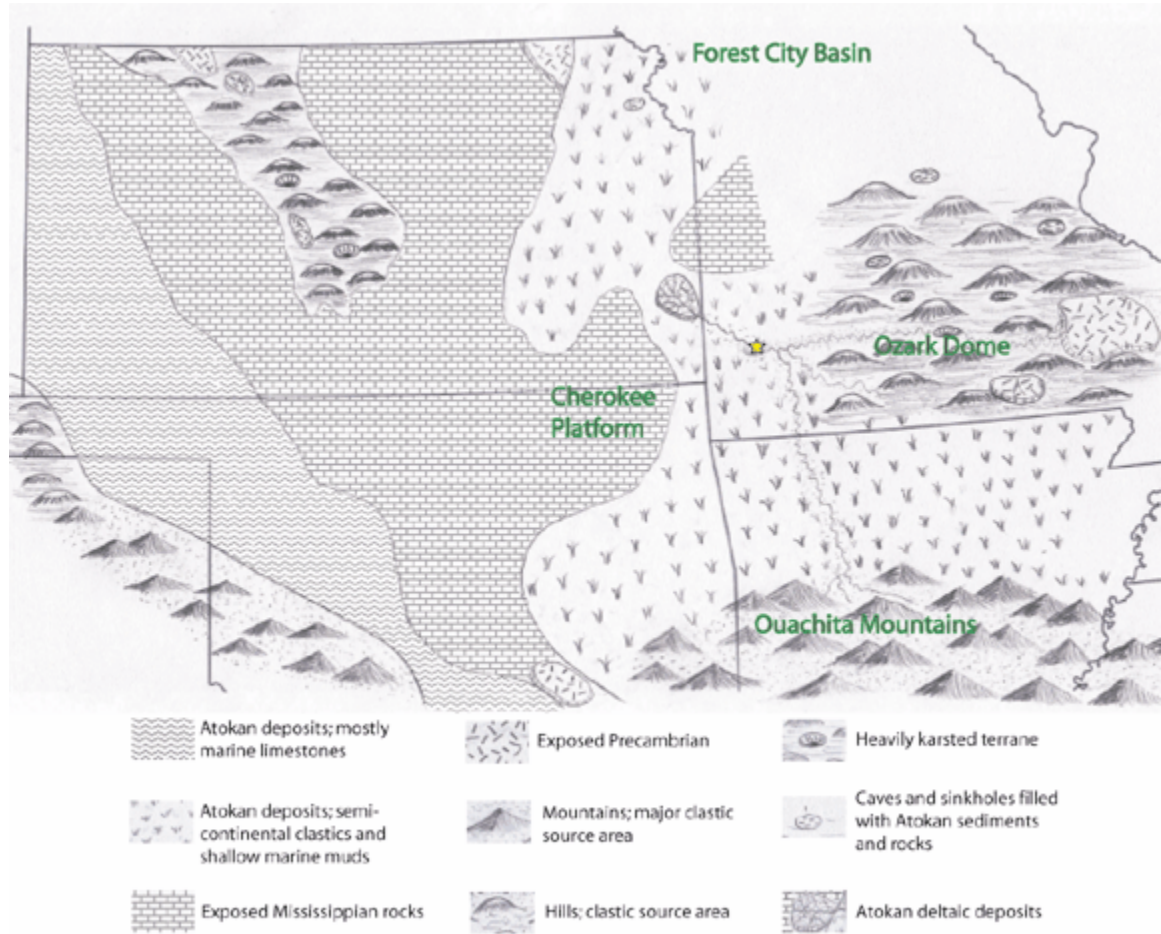


Figure 2.15. Late Atokan paleoterrain showing sediment sources for the cave-fills. The location of the delta is estimated but is likely on the eastern flank of the Forest City Basin. Modified from Rascoe and Adler (1983).



Figure 2.16. Generalized Late Atokan paleogeography modified from Blakey (2003).

## **Diagenesis**

### *Pyrite formation*

The pyrite in the slackwater facies is interpreted to have formed by early diagenesis, in the depositional environment, mediated by sulfate reducing bacteria. Organic carbon and detrital iron would have been plentiful in the environment; the limiting control on pyrite formation would have been dissolved sulfate (Berner, 1983). A source of dissolved sulfate may have come from plant ash (Canti 2003), suggested to be in the cave-fill by the presence of charcoal, and from oxidation of detrital sulfides prior to burial (Ulrich et al., 1998).

### *Secondary sulfates*

Secondary sulfate minerals from the oxidation and acid-weathering of pyrite are also common as efflorescent crusts, alteration zones, and precipitants within this facies. These minerals were identified using X-ray diffraction. Euhedral selenite gypsum clusters are common between shale layers (Fig. 2.17) and gypsum crusts altering to melanterite line the cave-roof (Fig 2.18). Copiapite (Fig. 2.19) and jarosite (and likely other associated minerals depending on season) alteration layers are common towards the top of the fills. The acid-weathering of pyrite, and the resulting series of sulfate salts, in Pennsylvanian rocks is described by Joeckel et al. (2007). Copiapite is the most common sulfate salt on the south outcrop. This mineral is likely mistaken for elementary sulfur within coals (McCaughey, 1918). These mineral salts may be an environmental concern on account of their solubility, possibly adding dissolved metals to local water supplies (Nordstrom and Alpers, 1999; Joeckel et al., 2007), but is beyond the scope of this study.

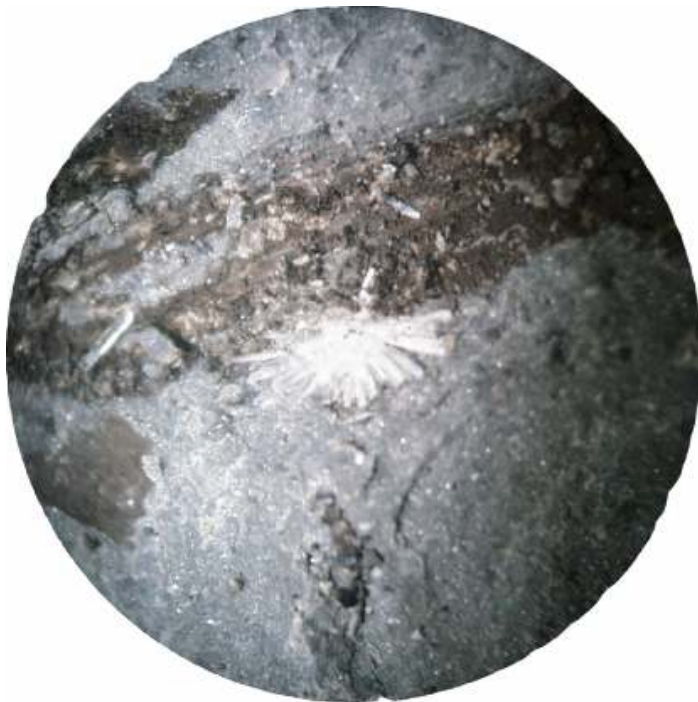


Figure 2.17. Selenite gypsum cluster between shale layers of the slackwater facies at 8X magnification. The black material is carbonized wood.

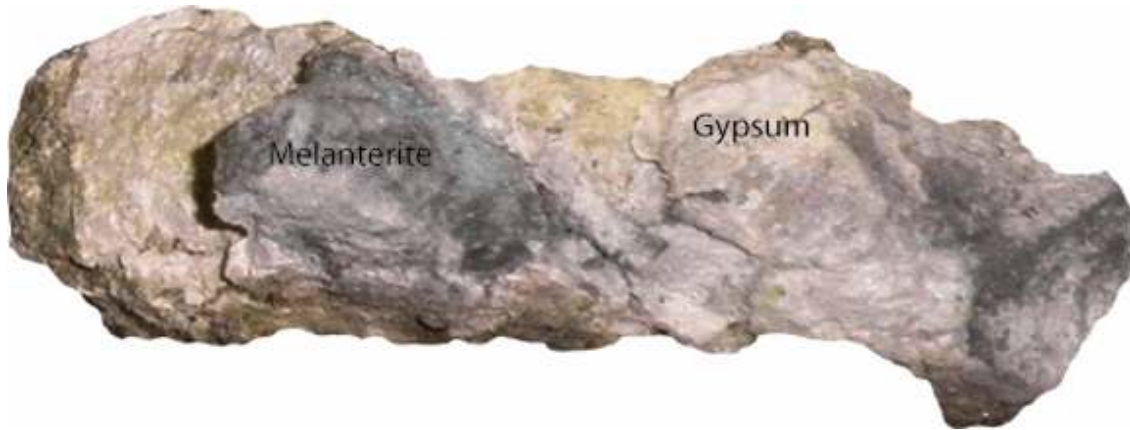


Figure 2.18. Gypsum crust from the cave-roof of the south cave-fill. Portions of the gypsum are altering to melanterite. Melanterite is the bluish silky fibrous mineral with the mineral formula  $\text{FeSO}_4 \cdot 7\text{H}_2\text{O}$ .



Figure 2.19. Copiapite from the south cave-fill. Copiapite is an easily soluble hydrated iron sulfate hydroxide mineral with the mineral formula  $\text{Fe}^{2+}\text{Fe}^{3+}_4(\text{SO}_4)_6(\text{OH})_2 \cdot 20(\text{H}_2\text{O})$ .

### *Secondary porosity*

The oxidation of pyrite is pertinent, however, because of the acidic solutions that result from this process and the secondary porosity it can create. Pyrite can oxidize in the subsurface from interactions with vadose or connate waters (Hutcheon, 1998; Ulrich, 1998; Tianfu, 2000). The resultant acidic solutions mostly dissolve carbonate cements,

interstitial material, and grains. This process may be the source of the secondary porosity observed in the cave-fill sandstones.

Measurements of sandstone porosity ranged from 8.5-17.2% and permeability ranged from 12.76-589.22 millidarcies. These two properties are correlative and are restricted by poor sorting (Fig. 2.20), interparticle hematite and organic-rich mud matrix material (Fig 2.21), as well as carbonate, quartz, clay, and hematite cements (Fig. 2.22). Some matrix material appears to have been replaced by carbonate cements. Quartz overgrowths are abundant in some samples and completely lacking in others. In several samples quartz overgrowths only appear on a few grains, which suggests that these grains were derived from reworked sandstone.

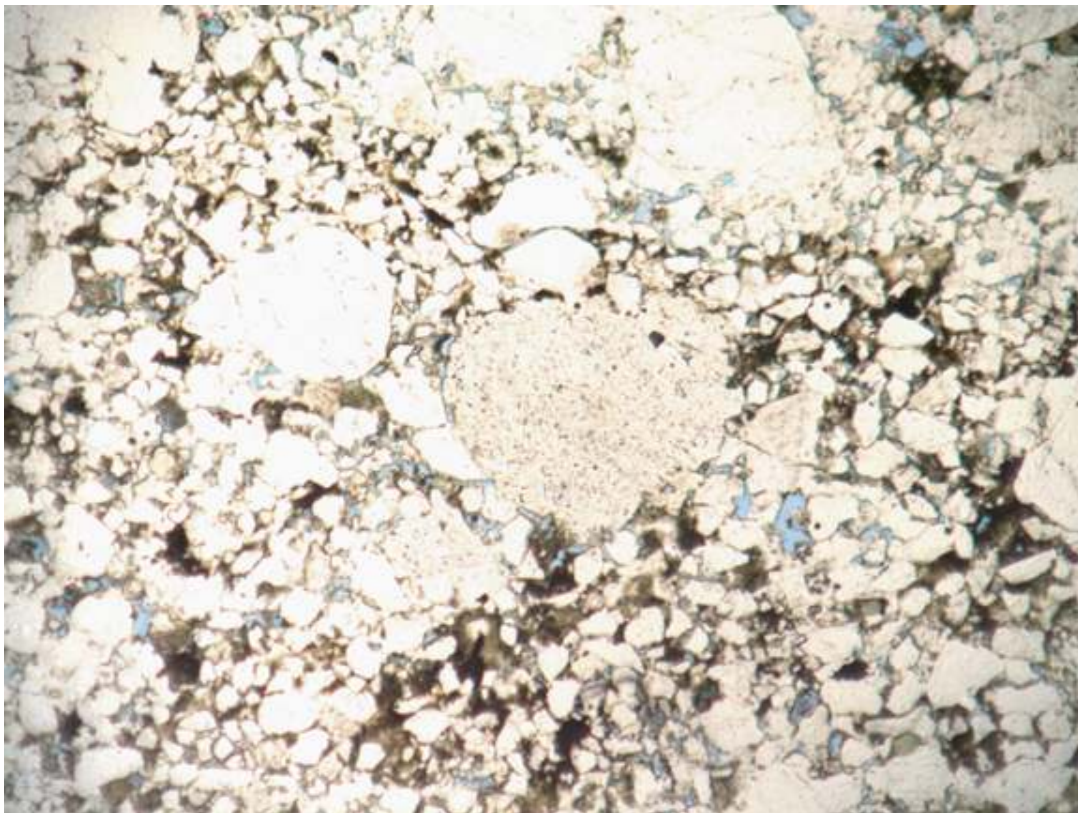


Figure 2.20. Sample E16. A poorly-sorted wacke with an estimated porosity of 9% and very low permeability. 20X magnification.

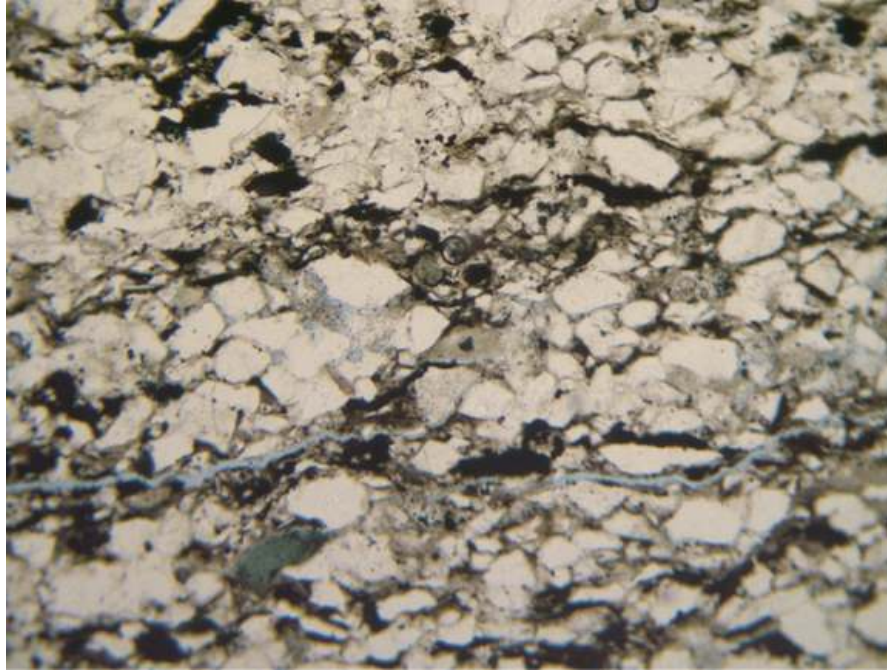


Figure 2.21. Sample W1. This sample has approximately 19% matrix material, 7% porosity, and very low permeability. The matrix material appears to be organic-rich mud. 80X magnification.

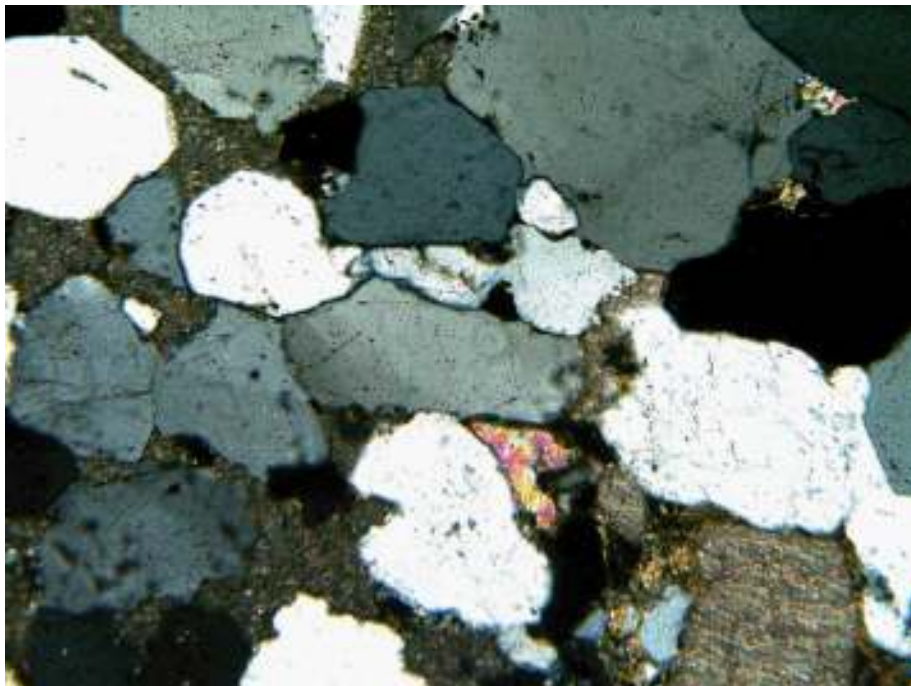


Figure 2.22. Sample E17. This sample is well cemented with carbonate cements. Other portions of this sample have high matrix content. This, and the floating grains suggest this cement is replacing the matrix material. This sample has 8.5% porosity and 12.76 millidarcies of permeability. 80X magnification.

Most of the porosity in the porous samples appears to be secondary. The secondary porosity in sandstones classification of Schmidt and McDonald (1979) was used for this study. The best evidence for secondary porosity includes moldic, oversized, and elongated pores, as well as corroded grains (Fig. 2.23) (Fig. 2.24) (Fig. 2.25). The oversized and elongated pores appear to be from the dissolution of unstable grains and matrix material. Corroded grains suggest this dissolution was caused by very acidic solutions, possibly derived from pyrite oxidation. Other types of porosity within the sandstone include primary or secondary intergranular and intraparticle porosity, as well as secondary shrinkage porosity from the alteration or dewatering of matrix material.

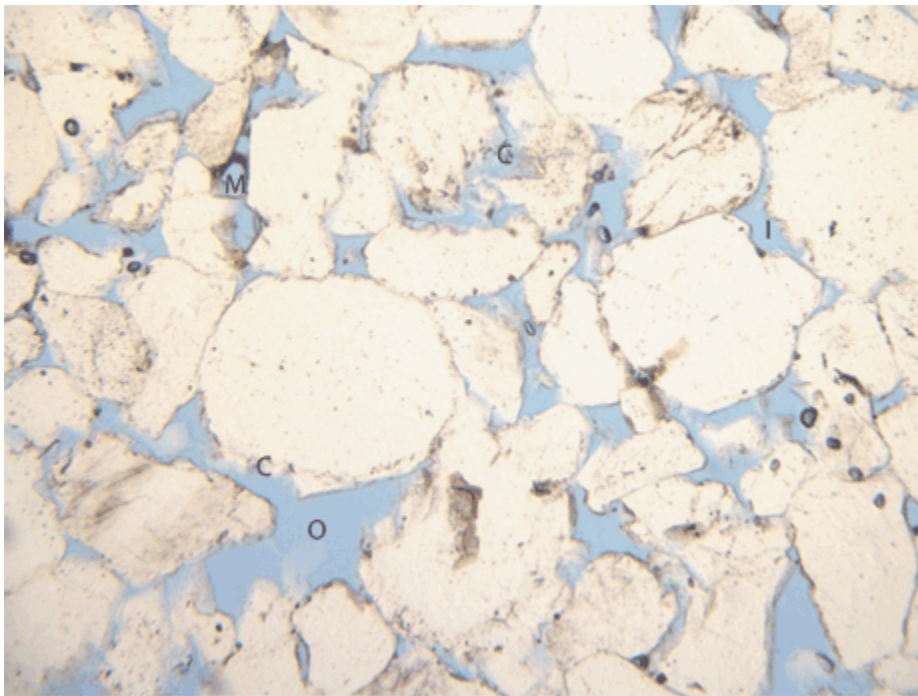


Figure 2.23. Sample E6. Approximately 15% porosity. Oversized pores (O) and corroded grains (C) are good evidence of secondary porosity. The corrosion of quartz grains suggest dissolution from a very acidic solution. Intergranular (I) and moldic (M) porosity is also present. 80X magnification.

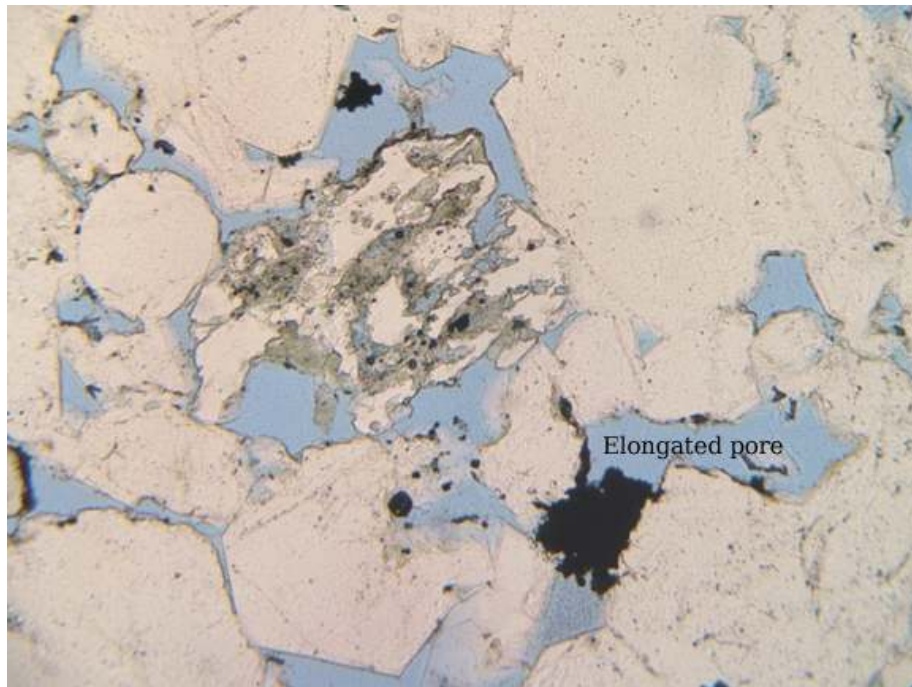


Figure 2.24. Sample W4 has 14.7% porosity and 206.55 millidarcies of permeability. The elongated pore is likely the result of the dissolution of matrix material. The altered grain in the center is microcline and has intraparticle porosity. 80X magnification.

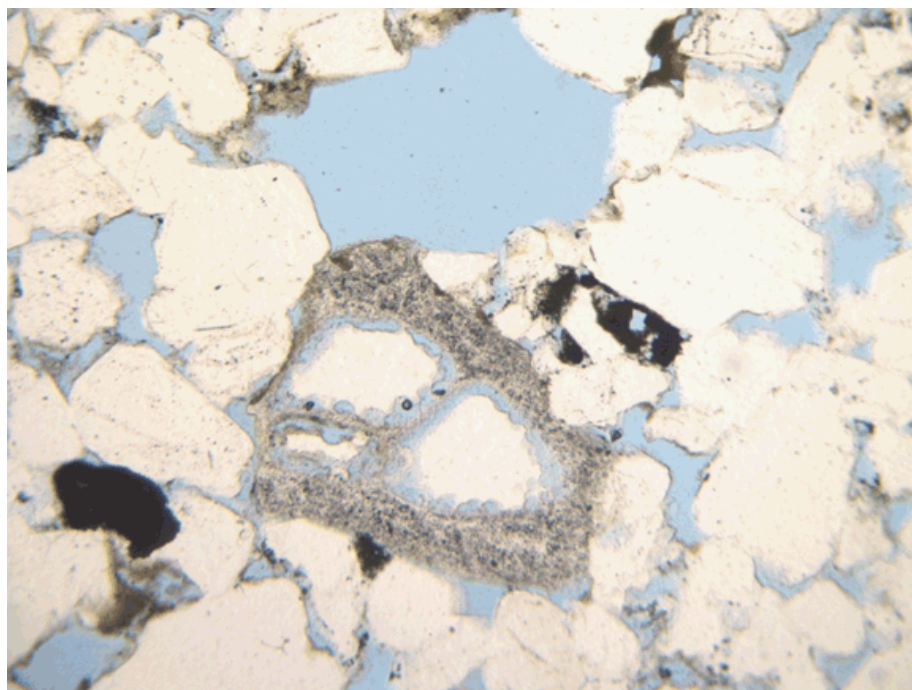


Figure 2.25. Sample E8 has approximately 15.5% porosity. The moldic pore in the middle is direct evidence of secondary porosity. 80X magnification.

## **Cave-System Hydrology and Geometry**

An extensive survey of epigenic caves (caves formed from meteoric water) by Palmer (1991) found that nearly all of these caves form along fractures or bedding planes. Water is concentrated into these small openings where dissolution takes place. When an opening becomes 5-10 mm in diameter it is considered a cave (Ford, 1988), at least hydraulically. A conduit which reaches this size can move a considerable volume of water and the influx of water undersaturated in respect to carbonate accelerates conduit growth progressively further into the cave-system (White, 1988). A conduit typically takes  $10^4 - 10^5$  years to become traversable (Palmer, 1991) and can theoretically last 1.25 – 10 Ma before denudation of the land surface unroofs and destroys the passage (Sasowsky, 2007). The study area was exposed approximately 13.9-19 Ma based on the International Commission on Stratigraphy's stratigraphic chart ([www.stratigraphy.org](http://www.stratigraphy.org), accessed October, 2011), enough time for a complex 3-D cave-network to form as local base levels changed.

The hydrology and geometry of the paleocave-system can be inferred by how the cave-fill was deposited. The recharge points of a cave-system (sinkholes, sinking streams, joints, fractures) dictate cave pattern whereas geologic structure and stratigraphy only influence orientation and extent (Palmer, 1991). The fluviokarst deposit is evidence of at least one sinking stream recharge point in this cave-system. Cave-systems recharged by sinking streams typically have rapid stage changes during storms. These subterranean streams differ from their surface counterparts in that flow is confined by the walls and sometimes the cave-roof, which makes pipe-full flow possible (Sasowsky,

2007). Backward or upward flow and sediment transport is even possible when the local base-level stream floods.

The southern cave-fill was recharged through a sinkhole or open fracture as suggested by its cave-fill. This cave-fill also contains collapse limestone boulders from the wall and roof of the cave imbedded in the fill. These boulders are in place due to the lack of active fluvial conditions in this passage to dissolve and carry these boulders downstream, hence the lack of cave-roof collapse boulders in the northern cave-fill.

The northern cave-passage recharged by the sinking stream may have grown at an accelerated rate due to its higher recharge. The southern paleocave likely grew slower because of its slower recharge. Passages of this type are more common, coalescing downstream forming higher order passages, and eventually join the main passage. This karst development leads to a branchwork cave-system with local anastomosing mazes and irregular networks (Fig 2.26). These types of caves are the most common (Palmer, 1991). Evidence of cave development along fractures suggests that many passages are angular, but local curvilinear passages along bedding plane partings are possible.

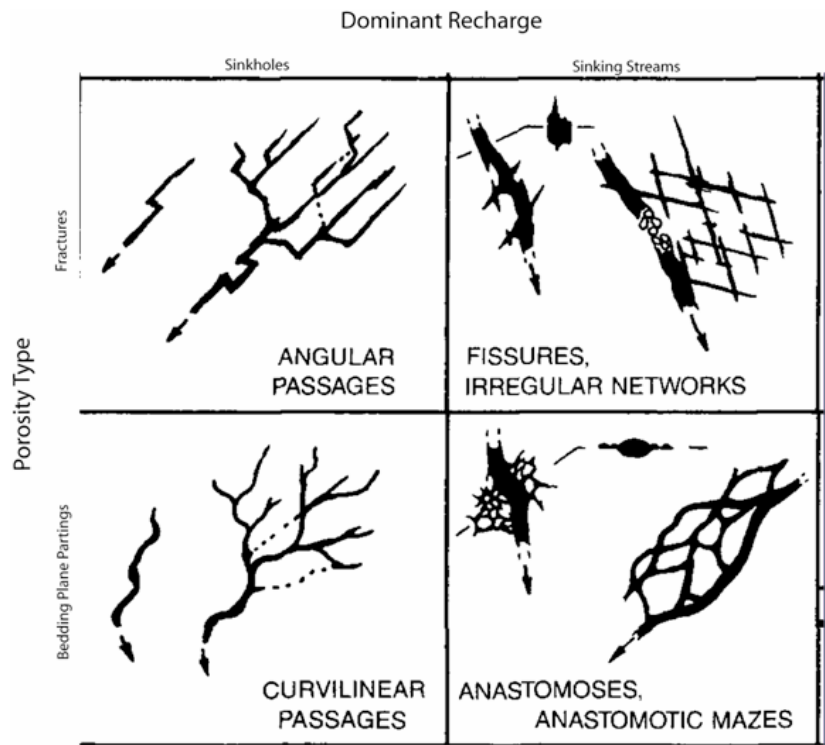


Figure 2.26. The most common cave-patterns observed in modern epigenic caves based on recharge and porosity type. Modified from Palmer (1991).

## **Chapter 3**

### **Cave-fill in pre-Absaroka caves in the Kansas subsurface**

#### **Pre-Absaroka cave formation in Kansas**

Although Kansas is not known for its caves today it was an ideal area for cave formation during the pre-Pennsylvanian hiatus. Several factors came together to make this possible:

- 1) The mid-continent was situated at about 10 degrees south latitude during this time (Gutschick and Sandberg, 1983). The climate was typically warm and moist, shown by extensive coal deposits within Pennsylvanian strata. Organic acid from the decay of plants and meteoric recharge therefore would have been plentiful for conduit enlargement.
- 2) This was a tectonically active time. The Central Kansas Uplift and Nemaha Ridge, as well as the reactivation of numerous unnamed basement features were uplifted in this period (Meriam, 1963). This uplift created fractures, faults, and dipping beds in Mississippian rocks into which meteoric water flowed.
- 3) The Mississippian and Ordovician carbonates that were exposed during this time are generally much thicker bedded than Cretaceous, Permian, and Pennsylvanian carbonates that are exposed now. The maximum width of a cave-passage is dependent on the thickness of the bed forming the cave-roof (White, 1988). Pre-Pennsylvanian caves within Mississippian carbonates in Kansas should be as extensive as modern caves forming within the same formations in the outcrop belt in Missouri and elsewhere.

## **Karst-controlled and cave-fill hydrocarbon reservoirs**

Karst-controlled reservoirs have been the targets of oil and gas exploration for decades and a list of references on such fields is given by Loucks (1999). Typically these reservoirs consist of collapsed cave-systems, creating a heterogeneous network of fractured and brecciated host-rock as well as open caverns. The cave-fill in these reservoir models are generally viewed as permeability barriers which contribute to the compartmentalization of hydrocarbon reservoirs (Kerans, 1988). Most cave-fill is indeed the impermeable slackwater facies described from the south cave-fill because the majority of caves are recharged through sinkholes. The northern cave-fill, however, suggests that sandstone cave-fill can transmit fluid and potentially be a hydrocarbon reservoir itself. Several small reservoirs in suspected cave-fill have indeed been located by a small survey of producing wells in Clark County, Kansas. These wells were reported as producing from the Mississippian but the rocks in which the wells produce from are not laterally traceable in any nearby wells.

### *Recognizing cave-fill in bore holes*

Recognition of cave-fill in drill-cuttings, cores, or electric logs is one way to postulate a possible cave-system when drilling in unexplored areas. Drill-cuttings of cave-fill are often mistaken for “cavings” by mud-loggers, as they often resemble the strata overlying the karsted formation. This was the case in the McLouth gas and oil field in Leavenworth and Jefferson Counties, Kansas, where cave-fill has been found in over half of the wells drilled and is found up to 150 feet below the Mississippian subcrop (Lee, 1944). The gamma-ray signature of cave-fill is often higher than the limestone host-rock, especially the clay-rich portion which includes the insoluble residues of the surrounding

limestone. The gamma-ray signature of the two cave-fills is shown in Figure 3.1 and an example of a suspected cave-fill from the subsurface is shown in Figure 3.2 and 3.3. The similarities of the gamma-ray log are noticeable.

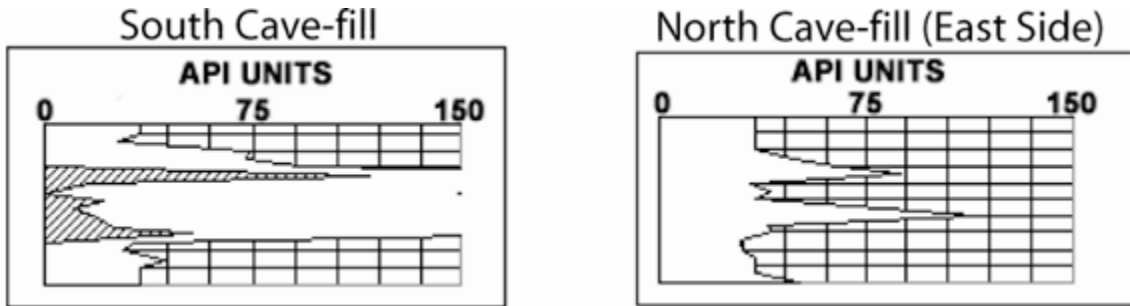


Figure 3.1. Gamma-ray results of the cave-fill outcrops. The vertical scale is 2 feet per section.

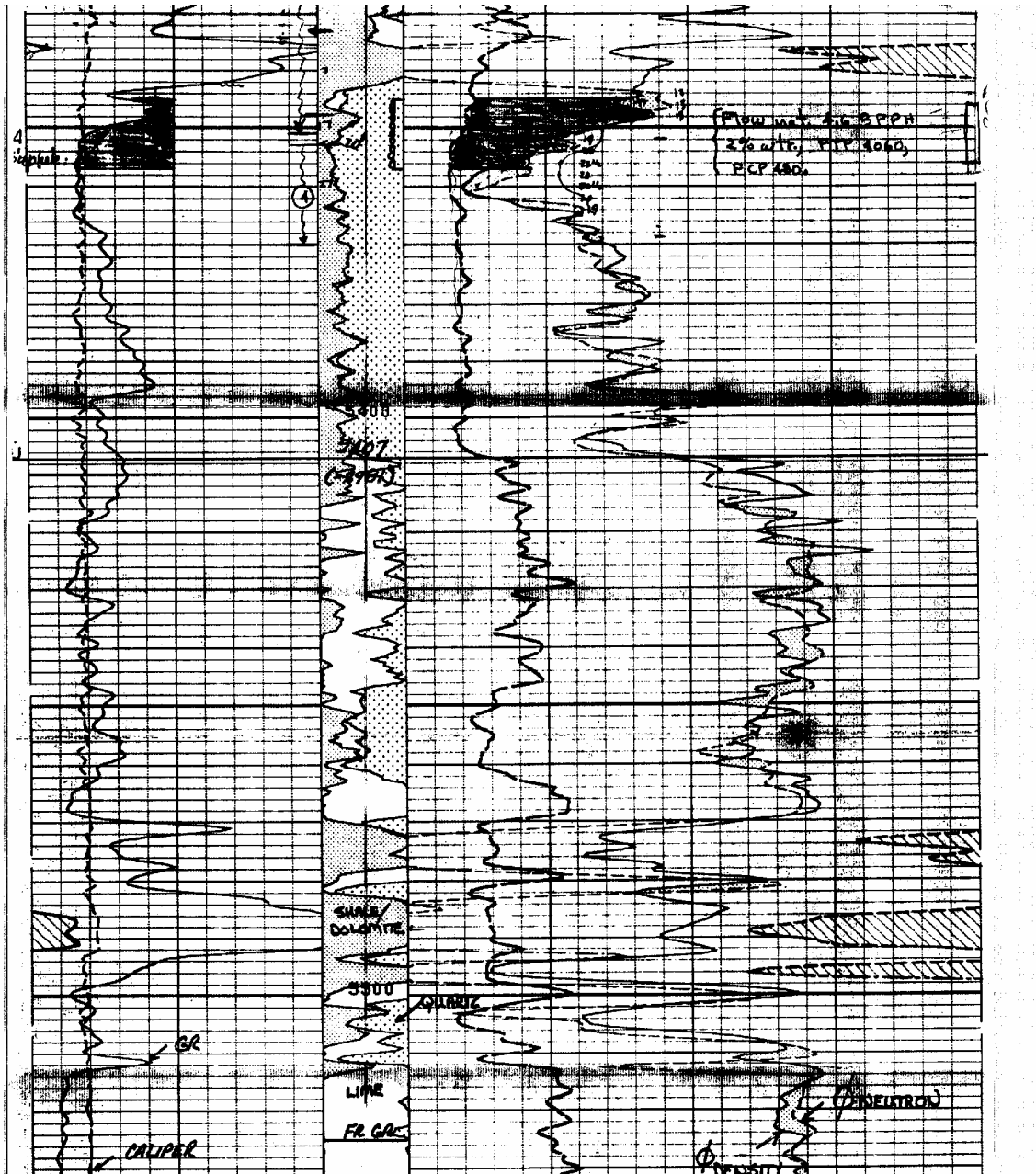


Figure 3.2. Suspected cave-fill shown on a gamma-ray/neutron-density porosity log from sec. 10-32S-22W (Clark County, Kansas). The top of the Mississippian is at a depth of 5407'. The cave-fill is sand and shale and was encountered from 5470' to 5512'.

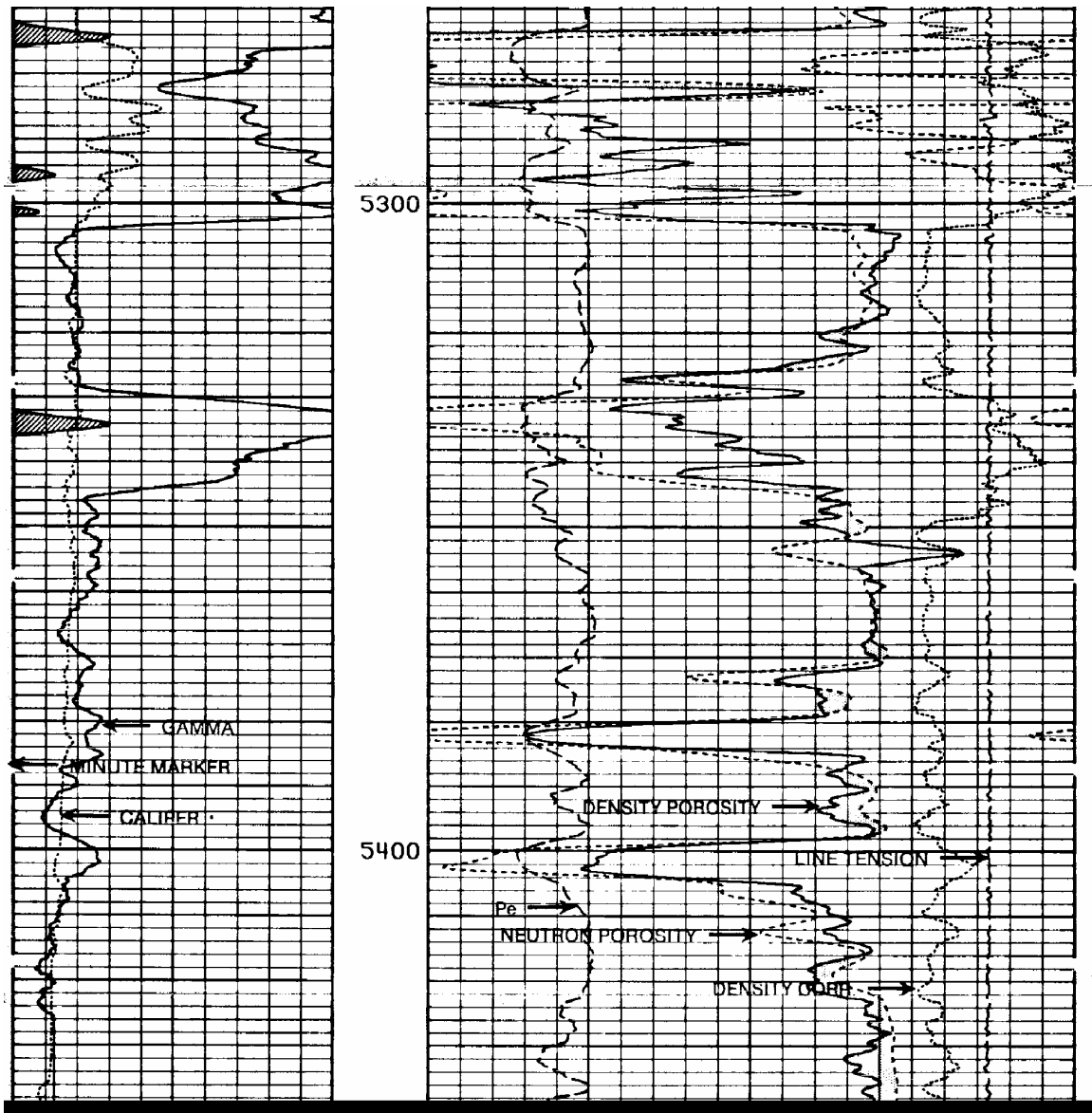


Figure 3.3. Suspected cave-fill from sec. 9-30S-22W (Clark County, Kansas). The top of the Mississippian is at a depth of 5303' and the cave-fill is at 5330'. The cave-roof and fill were perforated in this well and treated with acid. The zone made approximately 18,000 barrels of oil.

### Subsurface mapping of paleokarst landscapes

Paleokarst landscapes are easily recognizable in areas with good well-control by constructing isopachs above the karsted surface and with palinspastic restorations of the karst topography. Densely karsted areas in the Mississippian subcrop are most common

along major basement lineament; these major basement faults can be detected using Bouguer gravity and magnetics (Nissen et al., 2006; Ramaker, 2006). Beserra (2008) suggested that pre-Pennsylvanian paleovalleys developed in the Mississippian subcrop are major pathways of oil migration, making cave-fill and collapsed karst ideal targets along major basement lineaments.

An example of paleogeographic maps showing Mississippian karst features along a major basement lineament first recognized by residual aeromagnetism (Gay, 1995) in Clark County, Kansas is shown in figures 3.4 and 3.5. These maps include a Cherokee Shale to Mississippian isopach and a restored Mississippian structure map. Sinkholes can be inferred by enclosed thick sections overlying the Mississippian subcrop on isopach maps or by enclosed lows on the restored Mississippian structure map. Apparent sinkholes within paleovalleys may suggest sinking streams (Sando, 1988). A log cross-section of a sinking stream is shown in Figure 3.6. Even subtle karst features, i.e. clay-fills and sinkholes, are evidence of a karst network since every recharge point into the subsurface must have a discharge point (White, 1988). Steep-sided valleys with an abrupt termination on one end, known as blind valleys, can be inferred as the discharge point from a cave-system.

An area of interest where a paleocave-system is likely to exist can be drawn between these recharge and discharge points. High resolution 3-D seismic interpretation of this area of interest may lead to better prediction of the fractured karst network (Guan, 2006). Coalesced collapsed cave-systems may remain the primary objective when drilling for karst-controlled reservoirs but sandstone cave-fill should not be overlooked. Shale-filled caves should be taken into consideration when drilling lateral well-bores

within Mississippian rocks. These cave-fills could be mistaken for shales overlying the Mississippian and lead to erroneous downward steering of the drill bit.

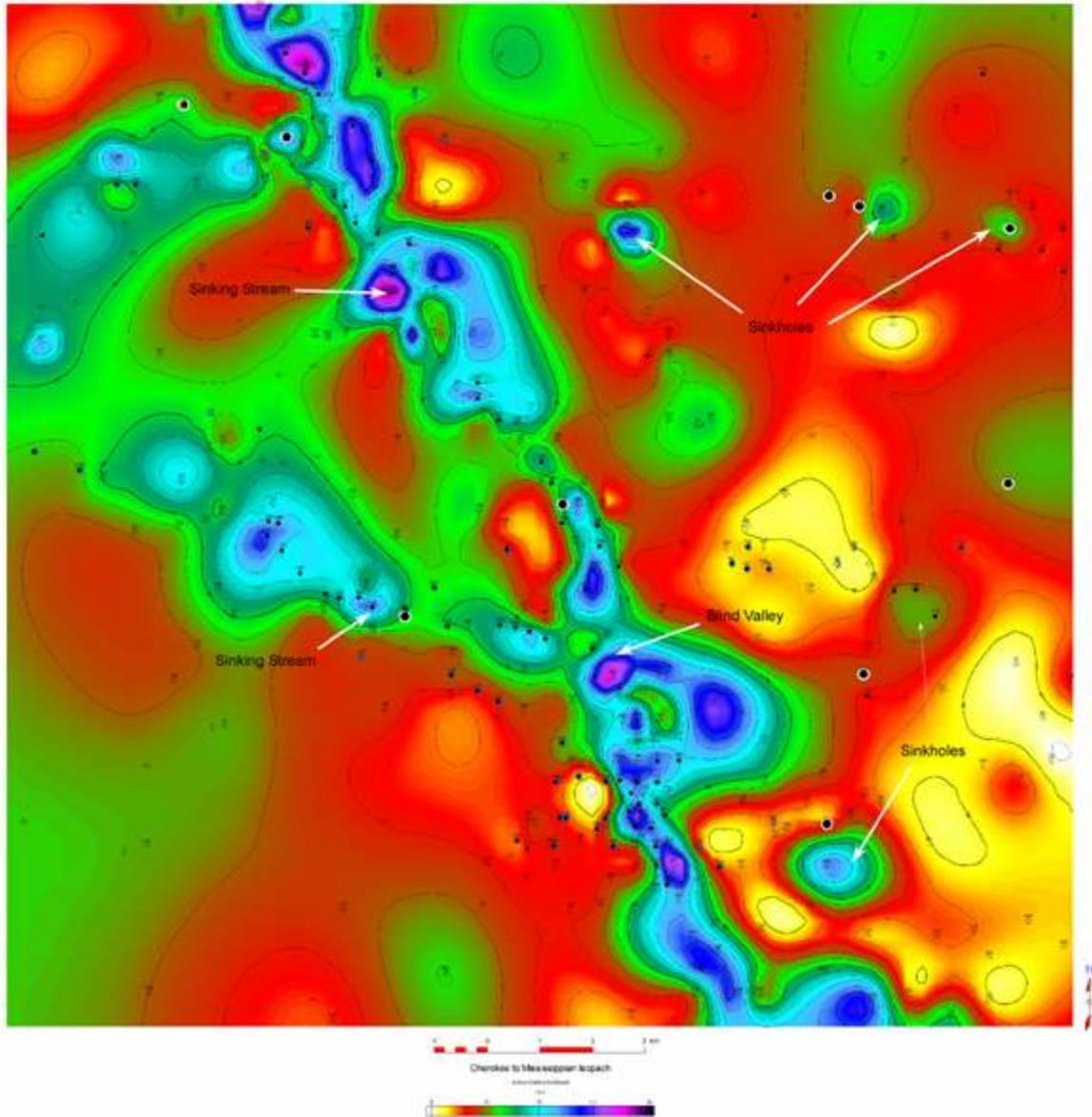


Figure 3.4. Cherokee to Mississippian isopach depicting karst recharge and discharge points. The blue/purple shades depict thick sections and clearly show paleovalleys. The thick sections enclosed by relatively thinner sections are inferred paleosinkholes. Abnormally thick sections within the paleovalleys may be sinking streams. Areas between sinkholes and the main NW-SE trending valley (the inferred discharge point of local paleocaves) are most likely to have developed cave-systems.

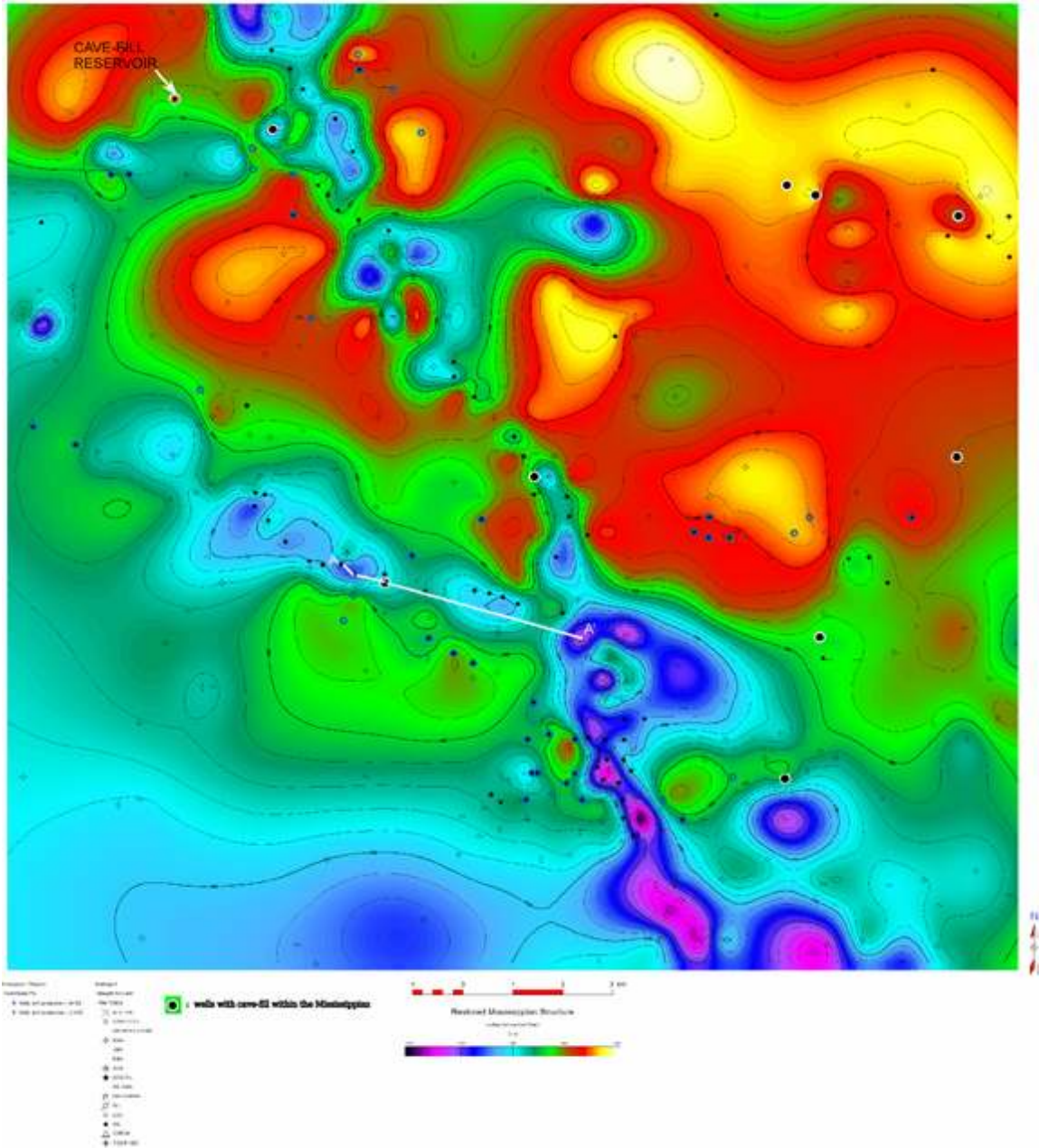


Figure 3.5. Restored Mississippian structure (Mississippian minus Stotler Fm. grid operation). This map shows the general dip direction of the paleosurface to the south-southwest; cave passages forming along bedding plane partings would likely be oriented this direction. The main fault on which the paleovalley is forming is trending north-northwest and secondary lineaments likely trend the same direction as the secondary channels; cave passages forming along fractures or faults would likely be oriented in the same directions as these basement lineaments. The well that produces from cave-fill (see Fig. 3.3) is shown on the upper left.

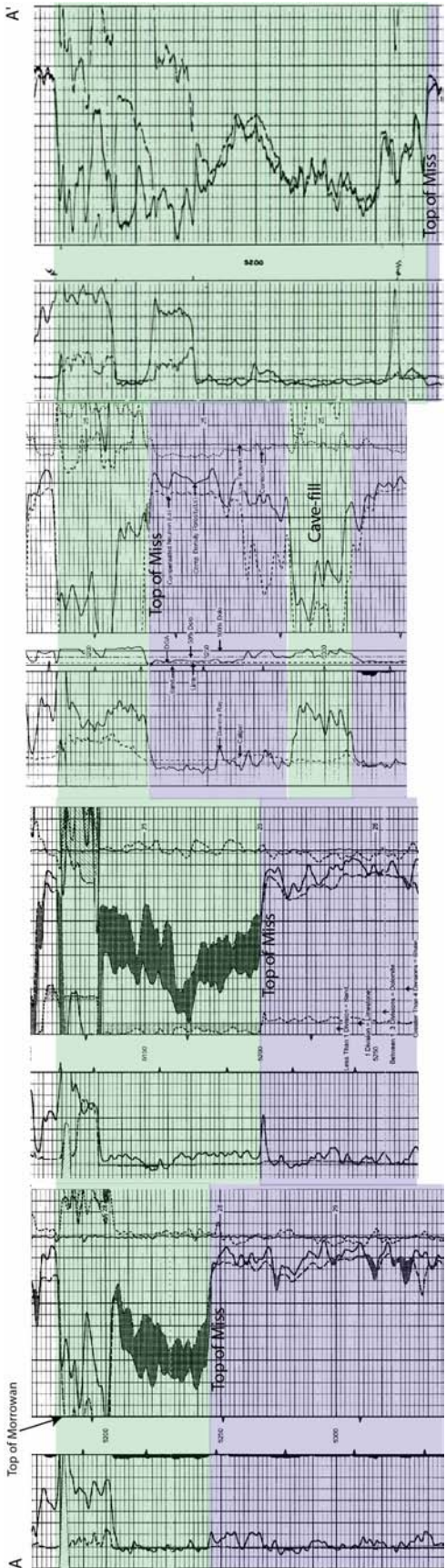


Figure 3.6. Gamma-ray/neutron-density porosity log cross-section A-A' shown on figure 3.5. The Morrowan-aged section is highlighted in green and the Mississippian-aged section is highlighted in blue. The logs are flattened on top of the Morrowan section to estimate the topography at the end of the pre-Pennsylvanian unconformity.

## **Chapter 4**

### **Conclusion**

The recently exposed paleocaves near South Greenfield in Dade County, Missouri, formed within the Osagean Burlington-Keokuk Limestone during the eustatic sea level drop marking the boundary between the Kaskaskia and Absaroka sequences. This event lasted from Late Mississippian to Middle Pennsylvanian time in southwest Missouri, a period of approximately 19 Ma. The paleocaves were located on the western flank of the Ozark Dome on the continent of Laurussia at approximately 10 degrees south latitude. The paleocaves, which consisted of two closely spaced large passages and several smaller conduits, are filled with Late Atokan siliciclastic terrestrial deposits.

The cave-fills consist of three lithofacies: the slackwater, channel, and diamictite facies. The slackwater facies consists of dark gray to black, sandy and silty, mudrock and shale that was deposited by stagnant water and some low energy currents. This sediment entered the cave-system via sinkholes, open fractures and joints, as well as by backflow during floods. This facies has experienced redox-conditions that ultimately led to the release of acidic solutions that were involved in the creation of secondary porosity. The channel facies is further divided into three subfacies based on texture. The lowest energy facies consists of flaser, wavy, and lenticular bedded silty very fine sandstone. The intermediate facies still consists of silty very fine sand, but lacks mud drapes. The high-energy facies consists of normal graded coarse to fine sand with varying amounts of matrix material. The channel facies was deposited during active fluvial conditions with sediment that entered the cave-system via a sinking stream. The diamictite facies

represents mass gravity flow deposits that were transported short distances from sinkhole collapses.

The northern cave-fill is comprised mostly of the channel facies whereas the south cave-fill consists mostly of the slackwater facies. The multiple recharge points of the paleocave system suggest a branchwork cave pattern. The pattern likely consisted of a few large passages that were recharged by the sinking stream and a multitude of smaller passages that were recharged by sinkholes. These passages likely developed along fractures and were linear with local anastomosing and curvilinear sections along bedding planes.

An abundance of metamorphic quartz grains, tripolitic spiculite, volcanic quartz, and reworked Chesterian fauna suggest a sandstone provenance from the Ozark Dome, Cherokee Platform, and Ouachita Mountains. Some cave sediments were derived locally from the overlying soil and regolith of the Burlington-Keokuk and authigenic sediments were derived from insoluble residues and limestone breakdown.

Climatic and tectonic conditions during the pre-Pennsylvanian unconformity were favorable for the formation of caves in Kansas and may influence Mississippian hydrocarbon production there. Cave-fill is usually overlooked as a petroleum reservoir target but measured porosity and permeability up to 17.2% and 589 millidarcies respectively suggest that the high-energy channel facies is a reservoir rock. Recognition of sinkholes, sinking streams, and blind-valleys on subsurface maps, as well as recognition of cave-fill on gamma-ray electric logs, can be used to hypothesize an area where a paleocave-system may exist within the Mississippian subcrop. Coalesced

collapsed caves remain the primary reservoir objective in karst reservoirs but sandstone cave-fill should not be overlooked as a potential target.

## **REFERENCES**

## REFERENCES

- Anthony, D.M., and Granger, D.E., 2006, Five million years of Appalachian landscape evolution preserved in cave sediments, in Harmon, R.S., and Wicks, C., eds., Perspectives on Karst Geomorphology, Hydrology, and Geochemistry – A Tribute Volume to Derek C. Ford and William B. White, Geological Society of America Special Paper no. 404, p. 39-50.
- Berner, R.A., 1983, Sedimentary pyrite formation: An update: *Geochimica et Cosmochimica Acta*, v. 48, p. 605-615.
- Beserra, T., et al., 2008, Oil classification and exploration opportunity in the Hugoton Embayment, Western Kansas, and Las Animas Arch, Eastern Colorado: Search and Discovery Article #10146.
- Bhattacharya, A., 1997, On the origin of non-tidal flaser bedding in point bar deposits of the river Ajay, Bihar and West Bengal, NE India: *Sedimentology*, v. 44, p. 973-975.
- Blakey, R.C., 2003, Carboniferous-Permian paleogeography of the assembly of Pangea: Proceedings of the XVth International Congress on Carboniferous and Permian stratigraphy, p. 443-456.
- Blatt, H., 1967, Provenance determinations and recycling of sediments: *J. Sed. Petrology*, v. 37, p. 1031-1044.
- Blatt, H., and Christie, J.M., 1963, Undulatory extinction in quartz of igneous and metamorphic rocks and its significance in provenance studies of sedimentary rocks: *J. Sed. Petrology*, v. 53, p. 559-579.
- Blatt, H., G.V. Middleton, and R.C. Murray, 1980, *Origin of Sedimentary Rocks*, 2<sup>nd</sup> ed., New York, Prentice Hall.
- Bosch, R.F., and White, W.B., 2004, Lithofacies and transport of clastic sediments in karstic aquifers, in Sasowsky, I.D., and Mylroie, J., eds., *Studies of Cave Sediments*: Kluwer Academics, New York, p.1-22.
- Bretz, J. H., 1950, Origin of the filled sink-structures and circle deposits of Missouri: *Geologic Society of America Bulletin*, v 61, p 789-834.
- Canti, M.G., 2003, Aspects of the chemical and microscopic characteristics of plant ashes found in archaeological soils: *Catena*, v. 54, p. 339-361.
- Ebanks, W.J., 1979, Correlation of Cherokee (Desmoinesian) sandstones of the Missouri-Kansas-Oklahoma tri-state area: in Hyne, N.J. eds., *Pennsylvanian Sandstones of the Mid-Continent*: Tulsa Geological Society Special Publication, p. 295-312.

## REFERENCES

- Evans, J. E. and Reed, J. M., 2006, Pennsylvanian fluvial cave sediments in the Mississippian Leadville Limestone, southwestern Colorado, U.S.A.: *Mountain Geologist*, v 43, p 283-297.
- Folk, R.L., and Ward, W.C., 1957, Brazos River bar: A study in the significance of grain-size parameters: *Journal of Sedimentary Petrology*, v. 27, p. 3-26.
- Ford, D.C., 1988, Characteristics of dissolutional cave systems in carbonate rocks, in Paleokarst, James, N. P. and Choquette, P.W., eds., New York, Springer-Verlag, p. 25-57.
- Ford, D.C., and Williams, P.W., 1989, *Karst geomorphology and hydrology*: London, England, Unwin Hyman, 601 p.
- Gastaldo, R.A., Allen, G.P., and Huc, A.Y., 1995, The tidal character of fluvial sediments of the modern Mahakam River delta, Kalimantan, Indonesia: in Flemming, B.W., Bartholomae, A. eds., *Tidal Signatures of Modern and Ancient Sediments*. Special Publication of the International Association of Sedimentologists, v. 24, p. 171-181.
- Gay, Jr., S.P., 1995, Basement control of selected oil and gas fields in Kansas as determined by detailed residual aeromagnetic data: *Kansas Geological Survey Bulletin*, v. 237, p. 10-16.
- Glasspool, I. J., et al, 2009, An ultrastructural investigation of early Middle Pennsylvanian megaspores from the Illinois Basin, USA: *Review of Palaeobotony and Palynology*, v 156, p 62-78.
- Guan, L., Wang, S., and Zhu, H., 2006, Prediction of a fracture-cavern system in a carbonate reservoir: A case study from Tahe oil field, China: *The Leading Edge*, v. 25, n. 11, p. 1396-1400.
- Gutschick, R.C., and Sandberg, C.A., 1983, Mississippian continental margins of the conterminous United States, in D.J. Stanley and Moore G.T., eds., *The Shelfbreak: Critical Interface on Continental Margins*: SEPM Special Publications 33, p. 79-96.
- Heckel, P.H., 1986, Sea-level curve for Pennsylvanian Eustatic marine transgressive-regressive depositional cycles along mid-continent outcrop belt, North America: *Geology*, v. 14, p. 330-334.
- Hutcheon, I., 1998, The potential tole of pyrite oxidation in corrosion and reservoir souring: *Journal of Canadian Petroleum Technology*, v. 37, n. 1. p. 1-5.

## REFERENCES

- International Stratigraphic Chart: International Commission on Stratigraphy, [www.stratigraphy.org](http://www.stratigraphy.org), accessed October, 2011.
- James, N.P., and Choquette, P.W., 1988, *Paleokarst*: New York, Springer-Verlag, 416 p.
- Jennings, J.N., 1971, *Karst*: Cambridge, MA, MIT Press, 252 p.
- Jennings, J.N., 1985, *Karst geomorphology*: Oxford, Basil Blackwell, 293 p.
- Joeckel, R.M., Wally, K.D., Fischbein, S.A., and Hanson, P.R., 2007, Sulfate mineral paragenesis in Pennsylvanian rocks and the occurrence of slavikite in Nebraska: *Great Plains Research*, v. 17, p. 17-33.
- Kaufman, J., Cander, H.S., Daniels, L.D., and Meyers, W.J., 1988, Calcite cement stratigraphy and cementation history of the Burlington-Keokuk Formation (Mississippian), Illinois and Missouri: *Journal of Sedimentary Petrology*, v. 58, n. 2, p. 312-326.
- Kerans, C., 1988, Karst-controlled heterogeneity in Ellenburger Group carbonates of West Texas: *AAPG Bulletin*, v. 72, n. 10, p. 1160-1183.
- Kisvarsanyi, E.B., 1974, Operation basement: Buried Precambrian rocks of Missouri – their petrography and structure: *AAPG Bulletin*, v. 58, n. 4, p. 674-684.
- Lee, W., and Payne, T. G., 1944, McLouth gas and oil field, Jefferson and Leavenworth Counties, Kansas: *Kansas Geol. Survey, Bull.* 53, p. 1-193.
- Loucks, R. G. 1999, Paleocave carbonate reservoirs: Origins, burial-depth modifications, spatial complexity, and reservoir implications: *American Association of Petroleum Geologists Bulletin*, v 83, p 1795-1834.
- Martin, A.J., 2000, Flaser and wavy bedding in ephemeral streams: a modern and an ancient example: *Sedimentary Geology*, v. 136, p. 1-5.
- Mazzullo, S.J., Wilhite, B.W., and Woolsey, I.W., 2009, Petroleum reservoirs within a spiculite-dominated depositional sequence: Cowley Formation (Mississippian: Lower Carboniferous), south-central Kansas: *AAPG Bulletin*, v. 93, n. 12, p. 1649-1689.
- Mazzullo, S.J., et al., 2011, Lithostratigraphy and conodont biostratigraphy of the Kinderhookian to Osagean Series on the western flank of the Ozark Uplift: *Tulsa Geological Society Field Trip Guidebook*.
- Merriam, D. F., 1963, The geologic history of Kansas: *Kansas Geological Survey Bulletin*, v. 162, 317 p.

## REFERENCES

- McCaughey, W.J., 1918, Copiapite in coal: *The American Mineralogist*, v. 3, n. 8, p. 162-163.
- Nissen, S. E., Carr, T.R., and Marfurt, K.J., 2006, Using New 3-D Seismic attributes to identify subtle fracture trends in Mid-Continent Mississippian carbonate reservoirs: Dickman Field, Kansas: *Search and Discovery*, Article #40189.
- Nordstrom, D.K., and Alpers, C.N., 1999, Negative pH, efflorescent mineralogy, and consequences for environmental restoration at the Iron Mountain Superfund site, California: *Proceedings of the National Academy of Sciences of the United States of America* 96:3455-62.
- Palmer, A. N., 1991, Origin and morphology of limestone caves: *Geologic Society of America Bulletin*, v 103, p 1-21.
- Peppers, R.A., 1996, Palynological correlation of major Pennsylvanian (Middle and Upper Carboniferous) chronostratigraphic boundaries in the Illinois and other coal basins: *Geological Society of America Memoir*, v. 188, p. 1-111.
- Peppers, R.A. and Brady, L.L., 2007, Palynological correlation of Atokan and Lower Desmoinesian (Pennsylvanian) strata between the Illinois Basin and the Forest City Basin in eastern Kansas: *Current Research in Earth Sciences*, v 253 (1).
- Plotnick, R. E., et al, 2009, Pennsylvanian paleokarst and cave-fills from Northern Illinois, USA: A window into Late Carboniferous environments and landscapes: *Palaios*, v 24, p 627-637.
- Phillips, T. L., Peppers, R. A., and DiMichele, W. A., 1985, Stratigraphic and interregional changes in Pennsylvanian coal-swamp vegetation—environmental inferences; in, *Paleoclimatic Controls on Coal Resources of the Pennsylvanian System of North America*, T. L. Phillips and C. B. Cecil, eds.: *International Journal of Coal Geology*, v. 5, p. 43–110.
- Ramaker, B.J., 2006, Influence of Mississippian Karst Topography on Deposition of the Cherokee Group: Ness County, Kansas: University of Kansas, Master's thesis, 183 p.
- Rascoe, B., and Adler, F.J., 1983, Permo-Carboniferous hydrocarbon accumulations, Mid-continent, U.S.A.: *AAPG Bulletin*, v. 67, n.6, p.979-1001.
- Sando, W. J., 1988, Madison Limestone (Mississippian) paleokarst: A geologic synthesis, in *Paleokarst*, James, N. P. and Choquette, P.W., eds., New York, Springer-Verlag, p 256-277.

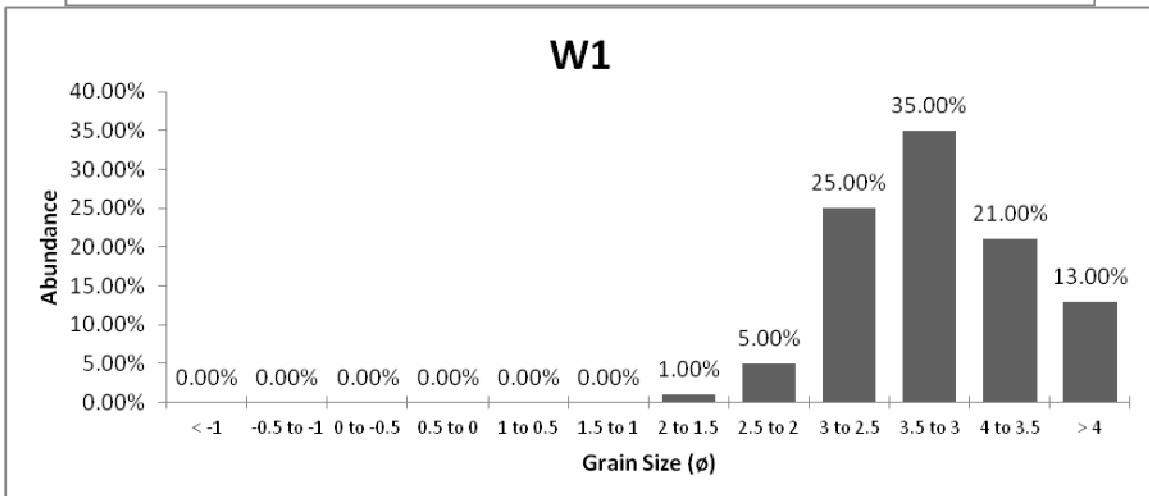
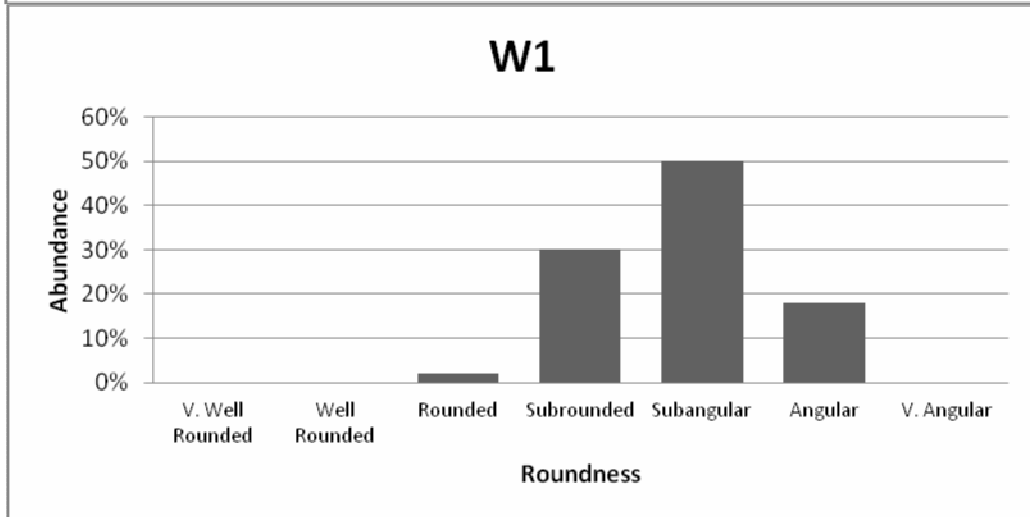
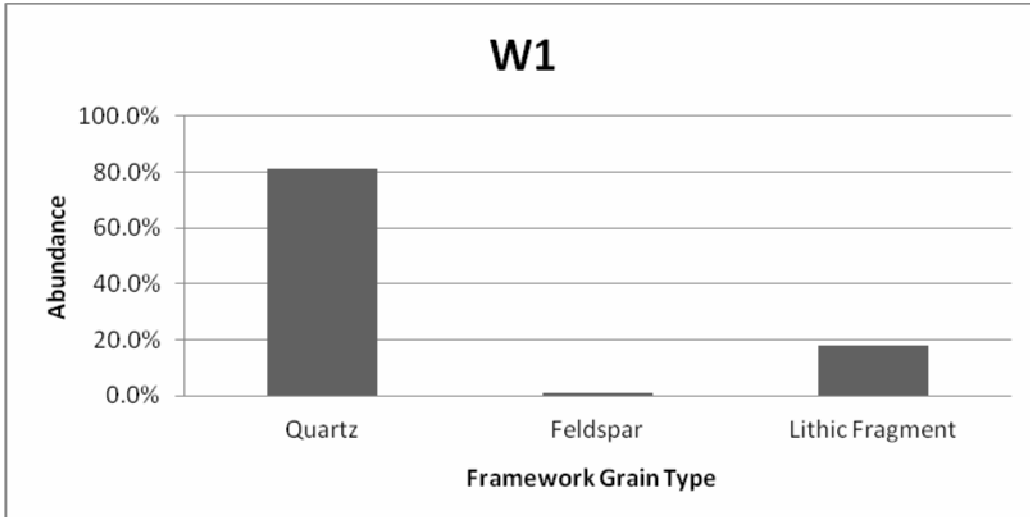
## REFERENCES

- Sasowsky, I. D., 2007, Clastic sediments in caves – imperfect recorders of processes in karst: *Acta Carsologica*, v 36/1, p143-149.
- Saunders, W.B. and Ramsbottom, W.H.C., 1986, The mid-Carboniferous Eustatic event: *Geology*, v. 14, p. 208-212.
- Schmidt, V., and McDonald, D.A., 1979, Texture and recognition of secondary porosity in sandstones: *Aspects of Diagenesis*, v. 26, p. 209-225.
- Seawright, W. V., and Howe, W. B., 1961, Pennsylvanian system in the stratigraphic succession in Missouri: J. W. Koenig (ed.) *Missouri Geological Survey and Water Resources*, Ser. 2, v. 40, p. 78-122.
- Sloss., L.L., 1963, Sequences in the cratonic interior of North America: *Geological Society of America Bulletin*, v. 74, p. 93-114.
- Tianfu, X., White, S.P., Pruess, K., and Brimhall, G.H., 2000, Modeling of pyrite oxidation in saturated and unsaturated subsurface flow systems: *Transport in Porous Media*, v. 39.1, p. 25-56.
- Ulrich, G.A., Martino, D., Burger, K., Routh, J., Grossman, E.L., Ammerman, J.W., Suflita, J.M., 1998, Sulfur cycling in the terrestrial subsurface: Commensal interactions, spatial scales, and microbial heterogeneity: *Microbial Ecology*, v. 36, p. 141-151.
- Veevers, J.J., and Powell, M., 1987, Late Paleozoic glacial episodes in Gondwana-land reflected in transgressive-regressive depositional sequences in Euramerica: *Geological Society of America Bulletin*, v. 98, p. 475-487.
- Wanless, H.R., J.R. Baroffio, J.C. Gamble, J.C. Horne, D.R. Orlopp, A. Rocha-Campos, P.C. Trescott, R.S. Vail, and C.R. Wright, 1970, Late Paleozoic deltas in the central and eastern United States, in, Morgan, J.P., ed., *Deltaic Sedimentation; Modern and Ancient: Soc. of Econ. Paleon. and Mineral. Spec. Publ. #15*, p. 215-245.
- White, W. B., 1988, *Geomorphology and hydrology of karst terrains*, Oxford University Press, p 464.
- Whiteside, D.I., and Marshall, J.E.A., 2008, The age, fauna and paleoenvironment of the Late Triassic fissure deposits of Tytherington, South Gloucestershire, UK: *Geological Magazine*, v. 145, p. 105-147.
- Zeller, D. E., 1968, The stratigraphic succession in Kansas: *Kansas Geol. Survey, Bull.*, v. 189.

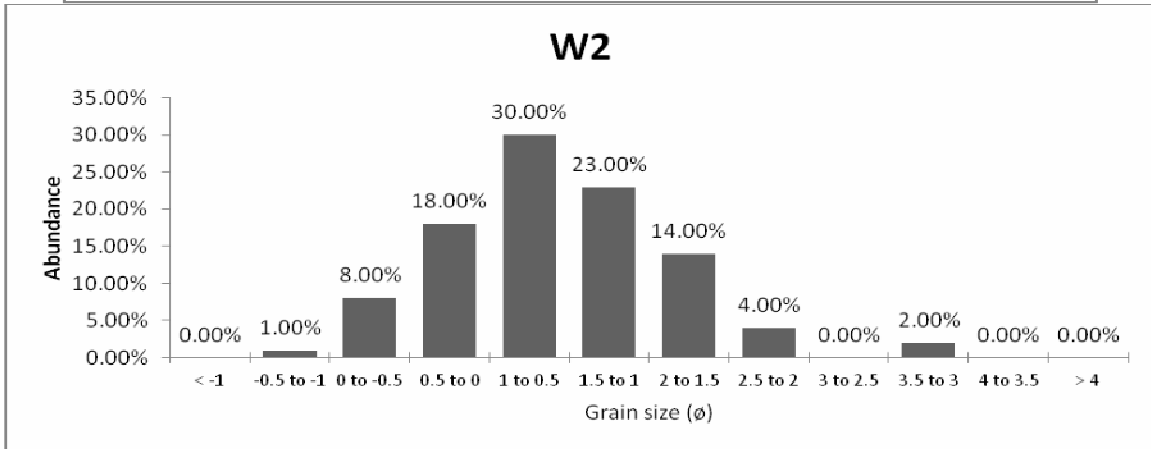
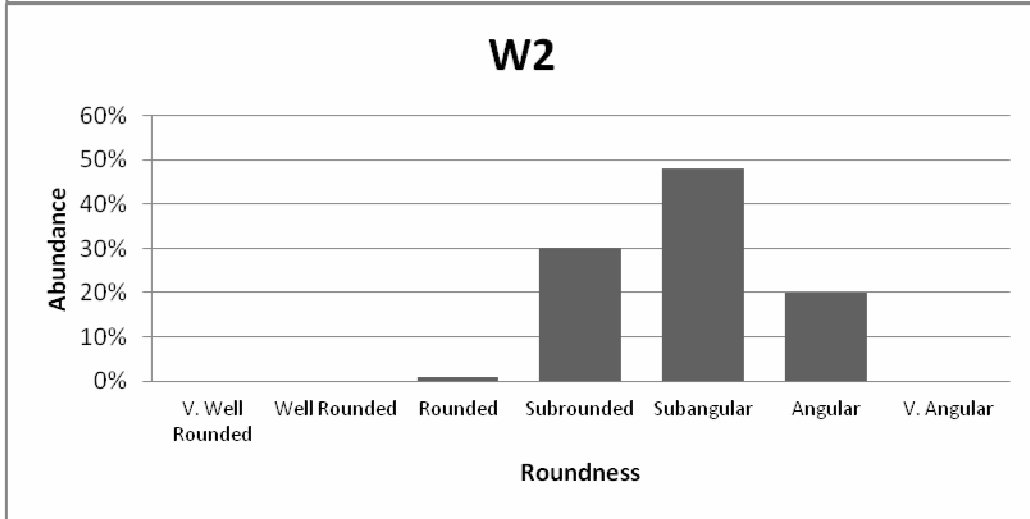
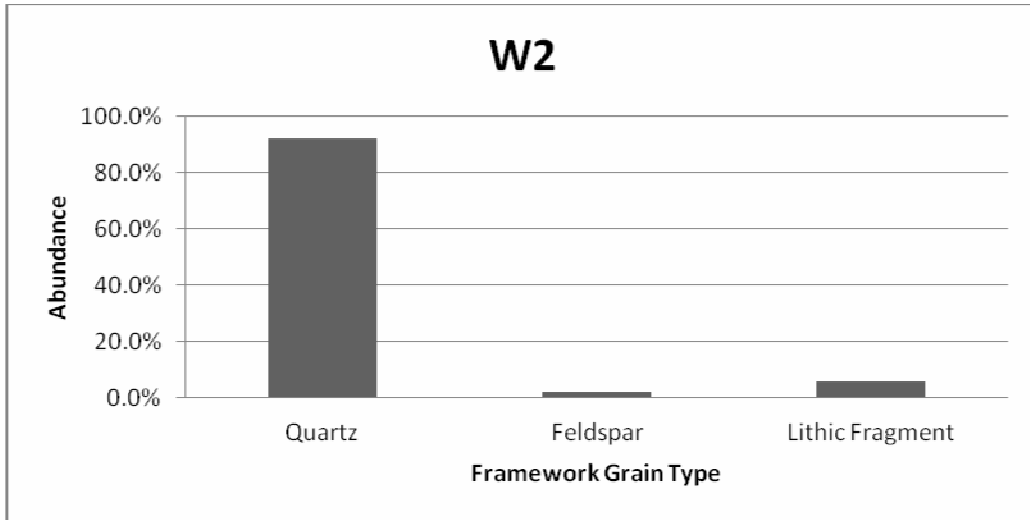
## **APPENDIXES**

**APPENDIX A:**

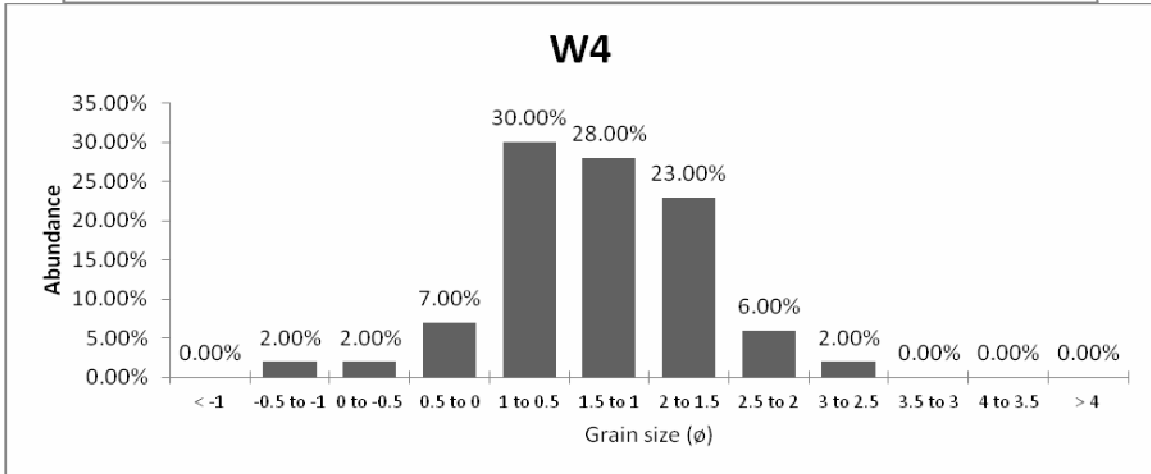
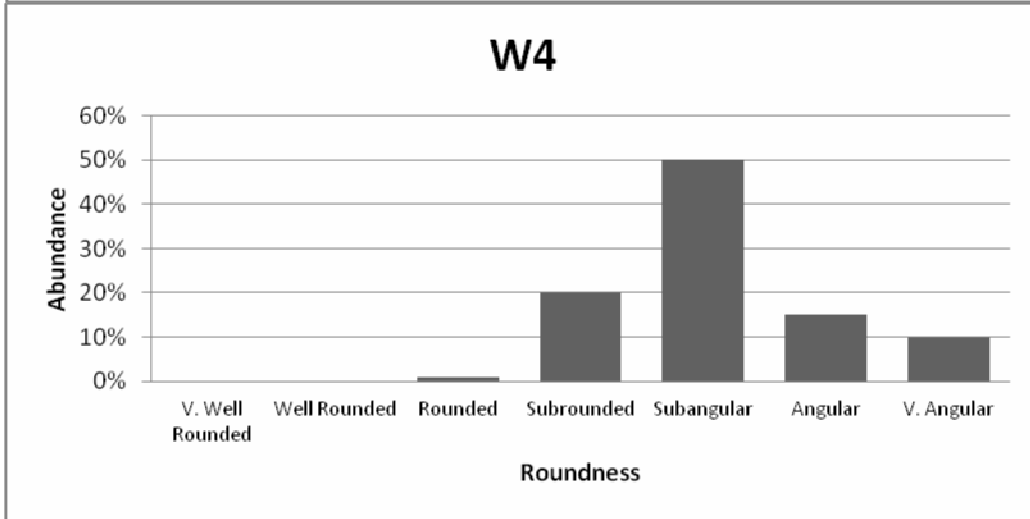
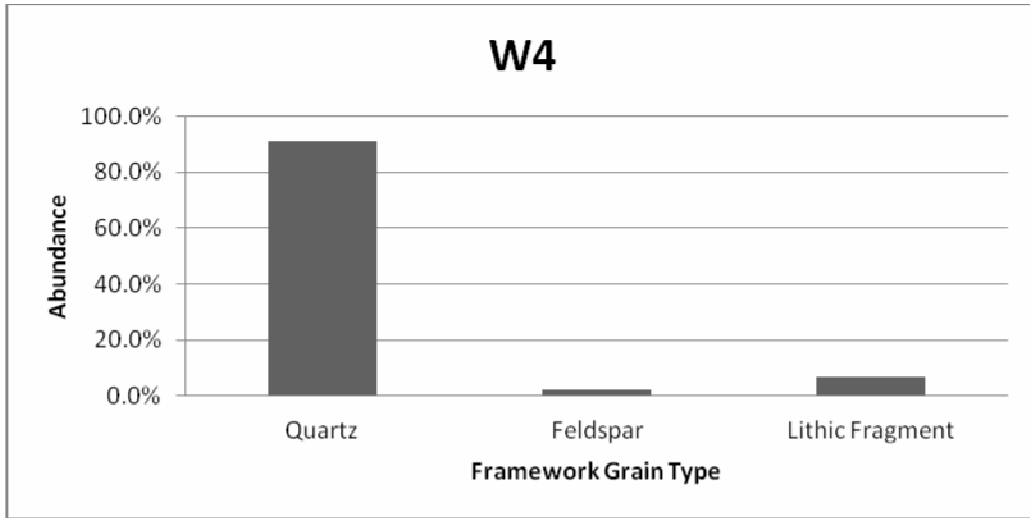
**SANDSTONE MINERALOGY, GRAIN-SIZE, AND TEXTURE**



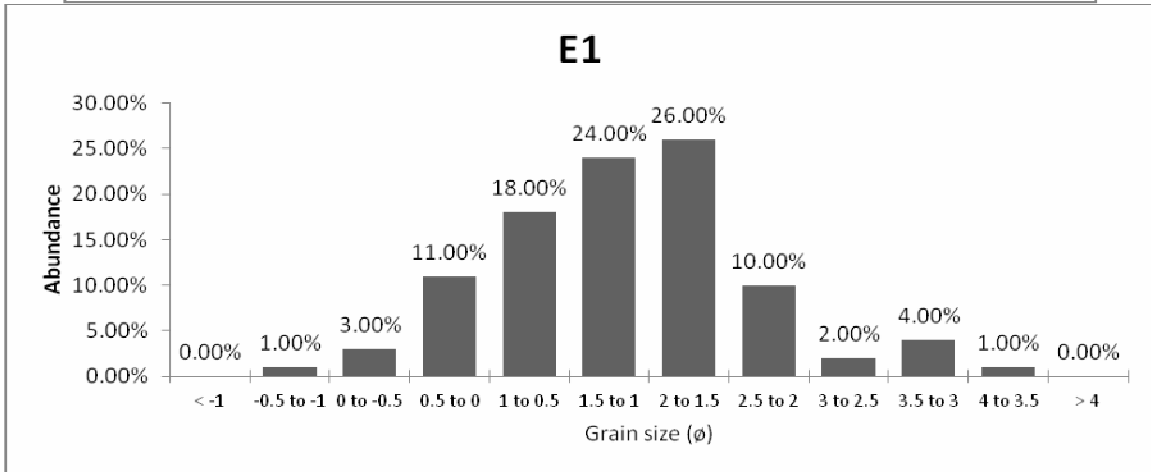
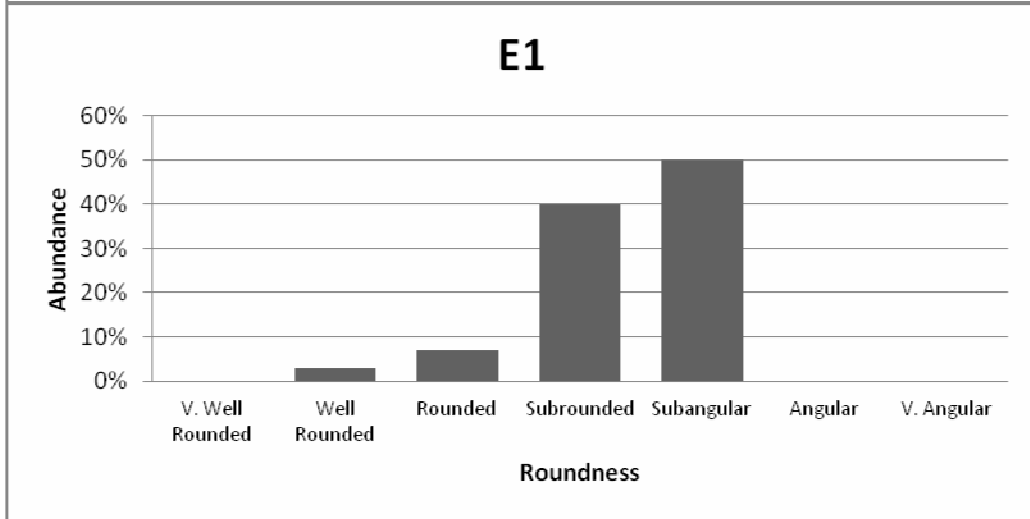
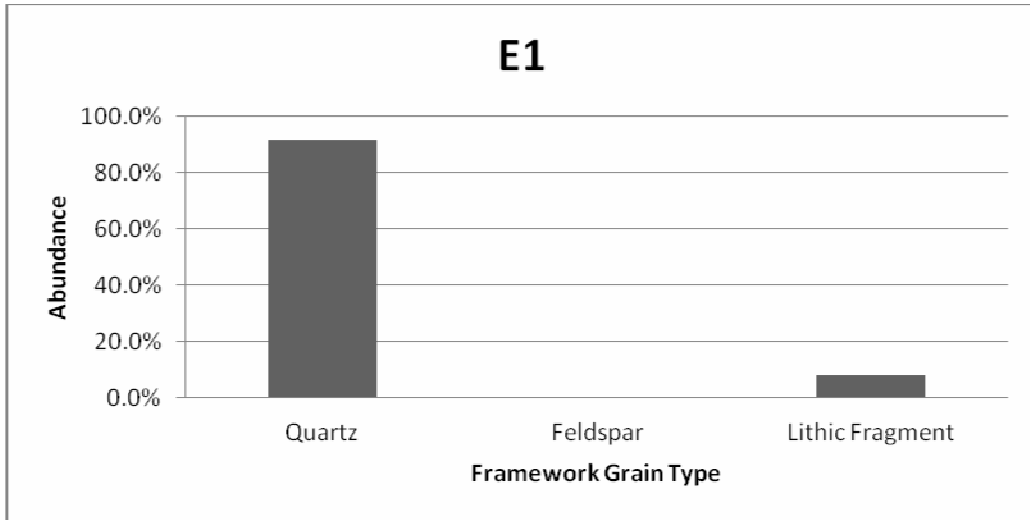
**APPENDIX A (continued)**



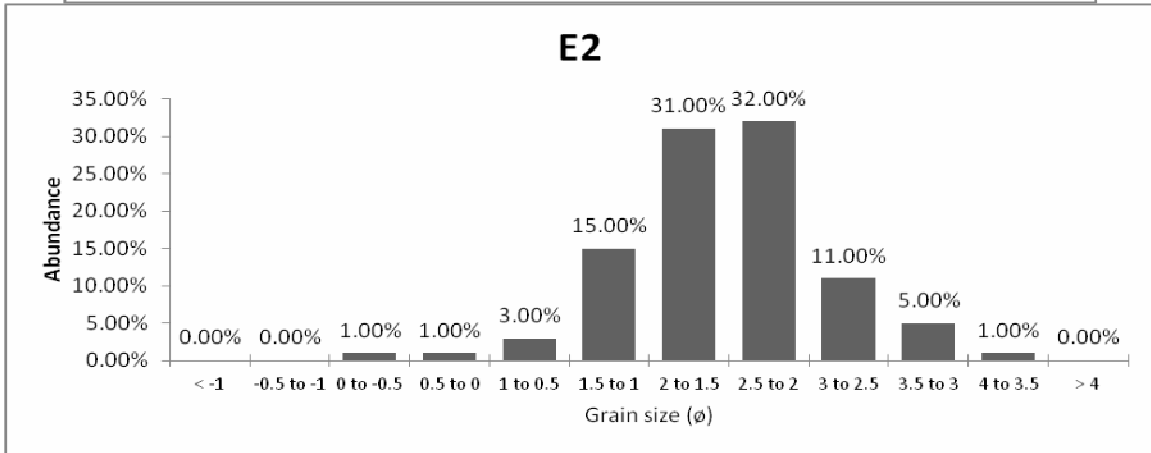
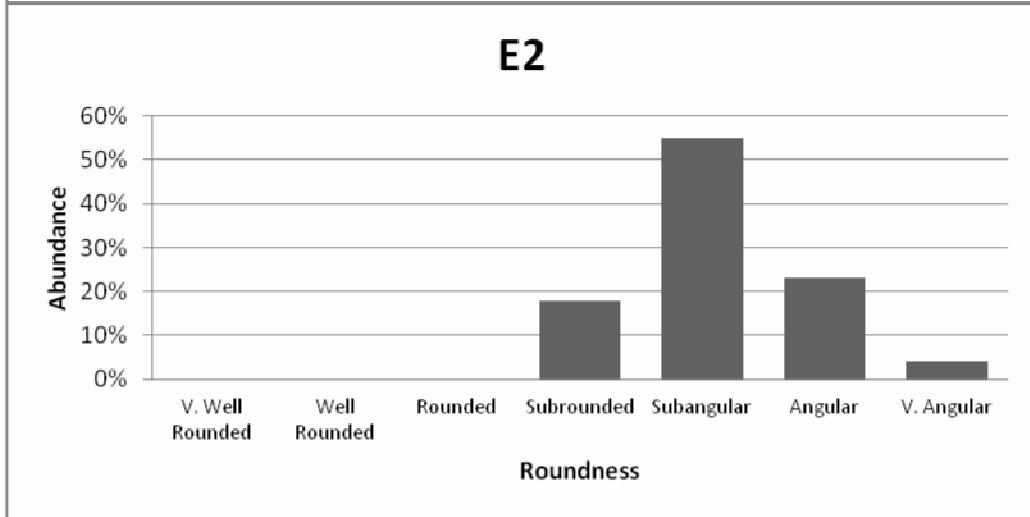
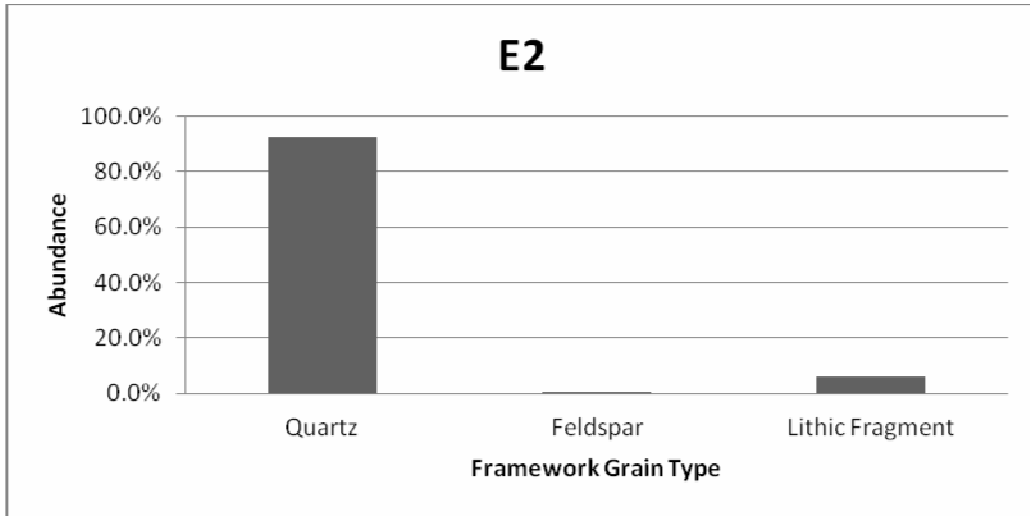
**APPENDIX A (continued)**



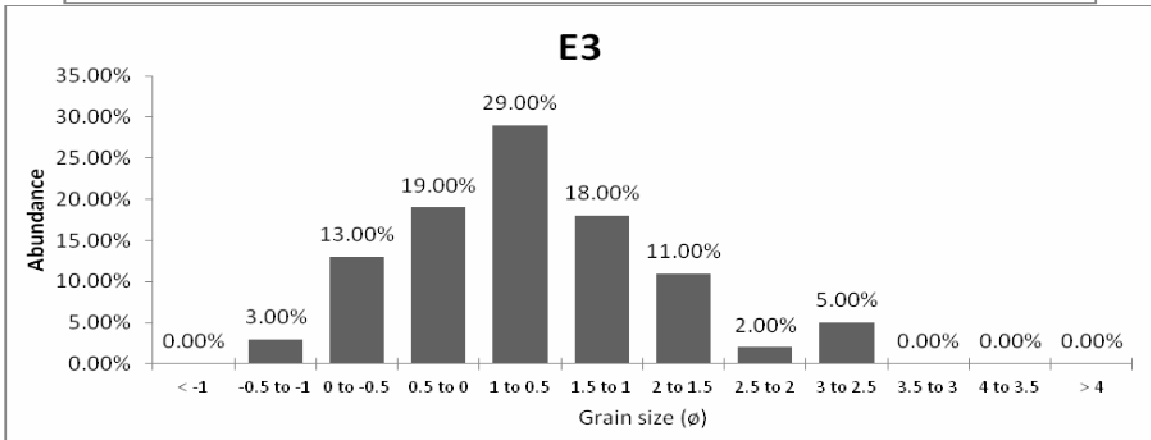
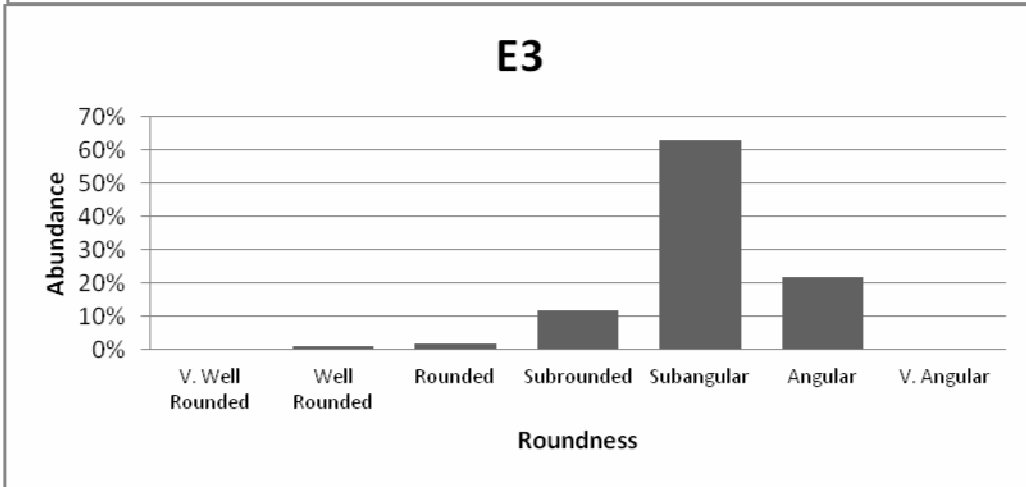
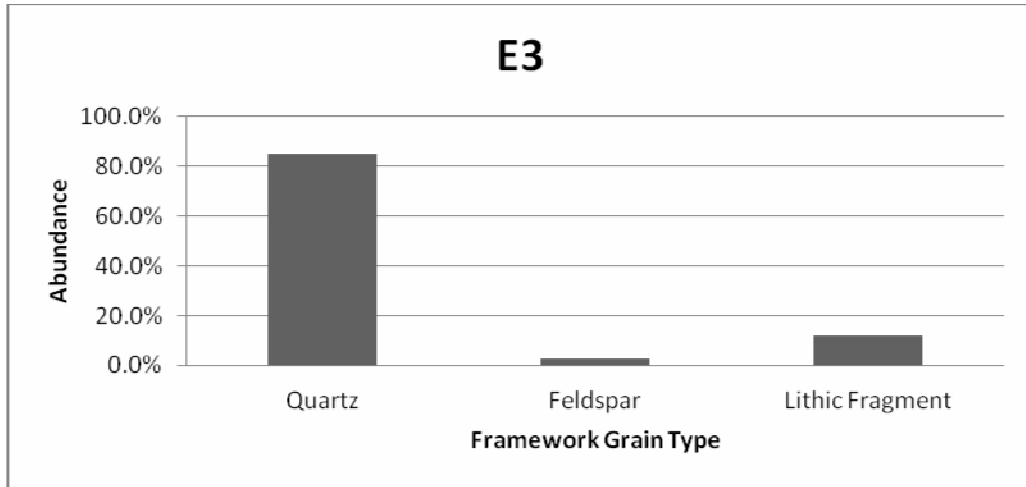
**APPENDIX A (continued)**



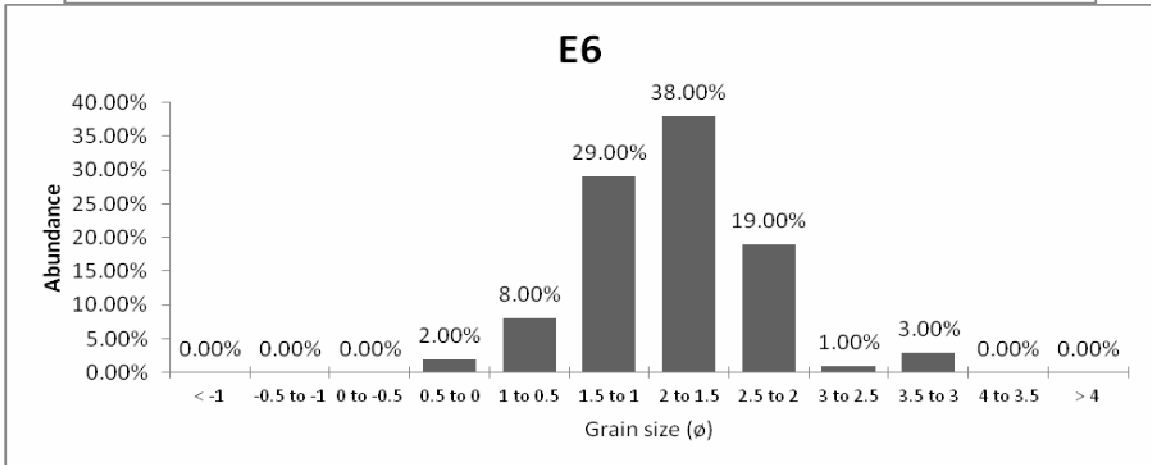
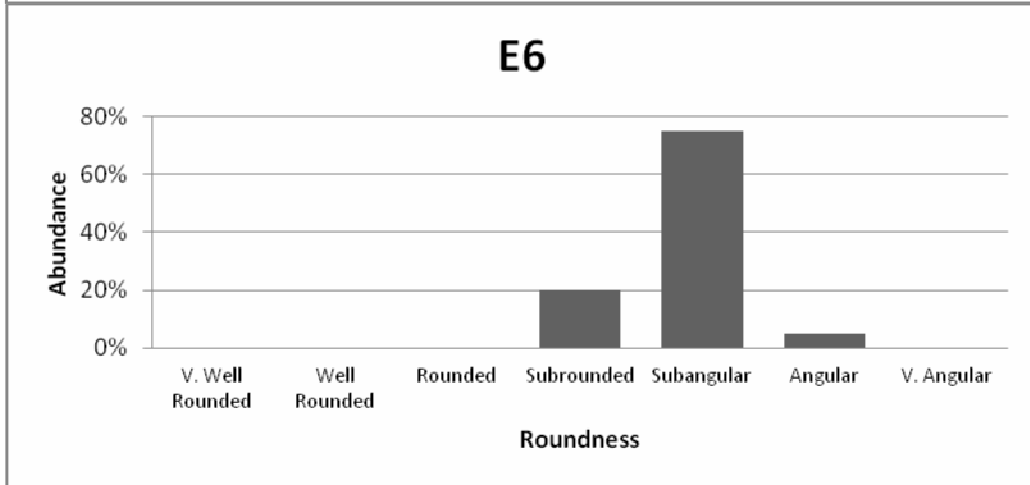
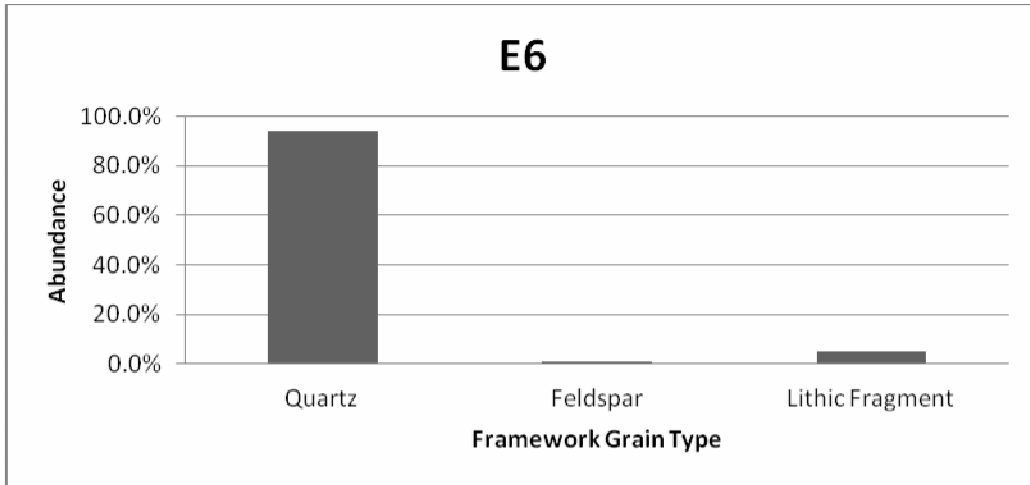
**APPENDIX A (continued)**



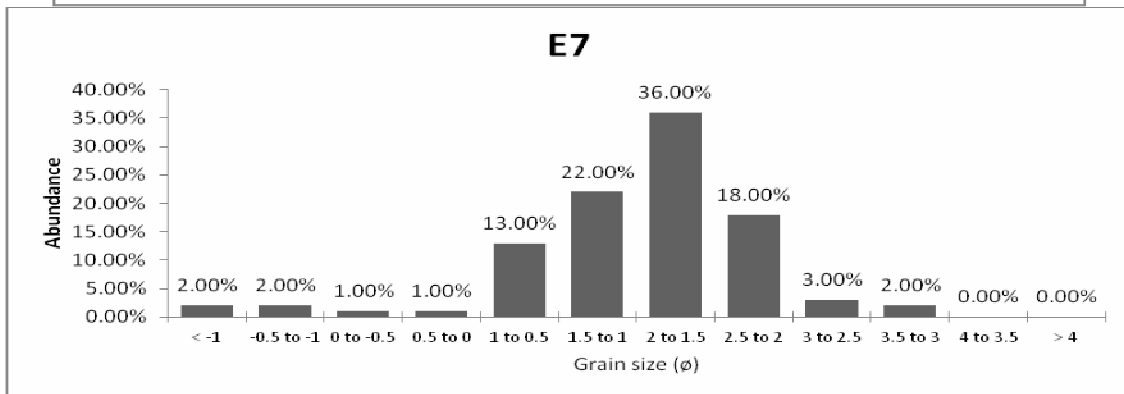
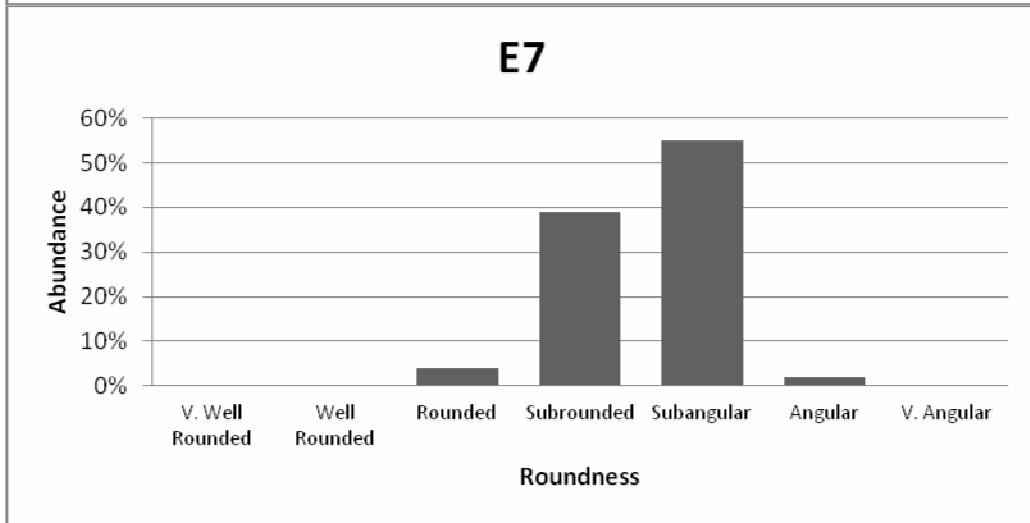
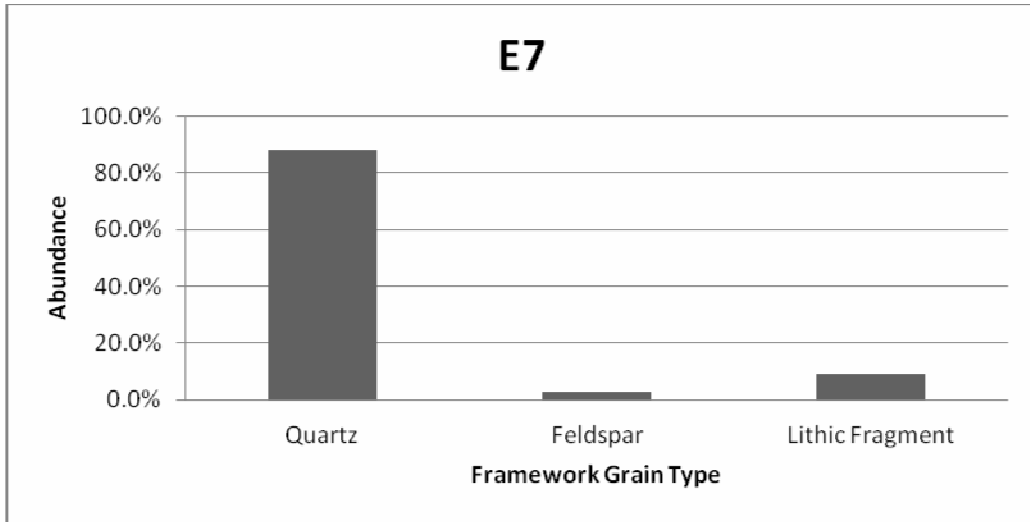
**APPENDIX A (continued)**



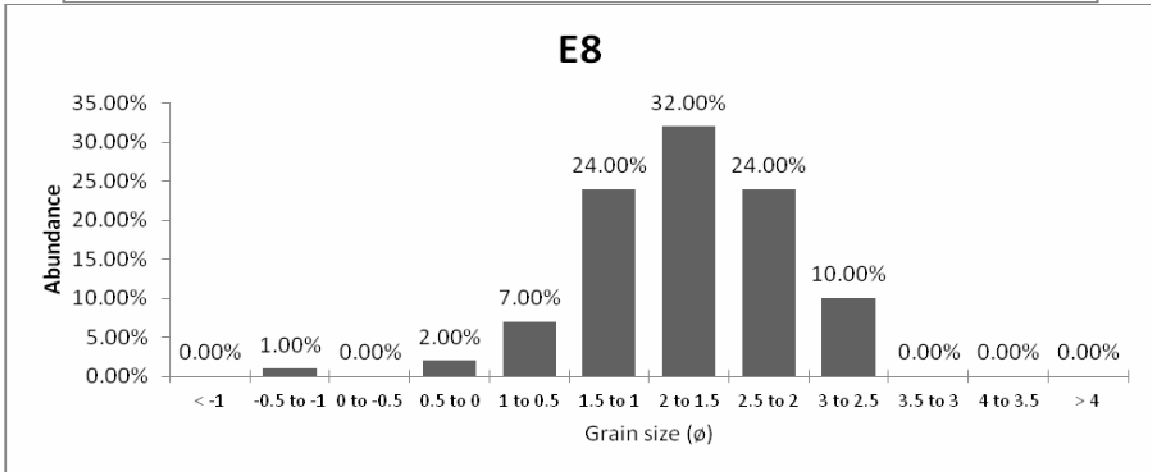
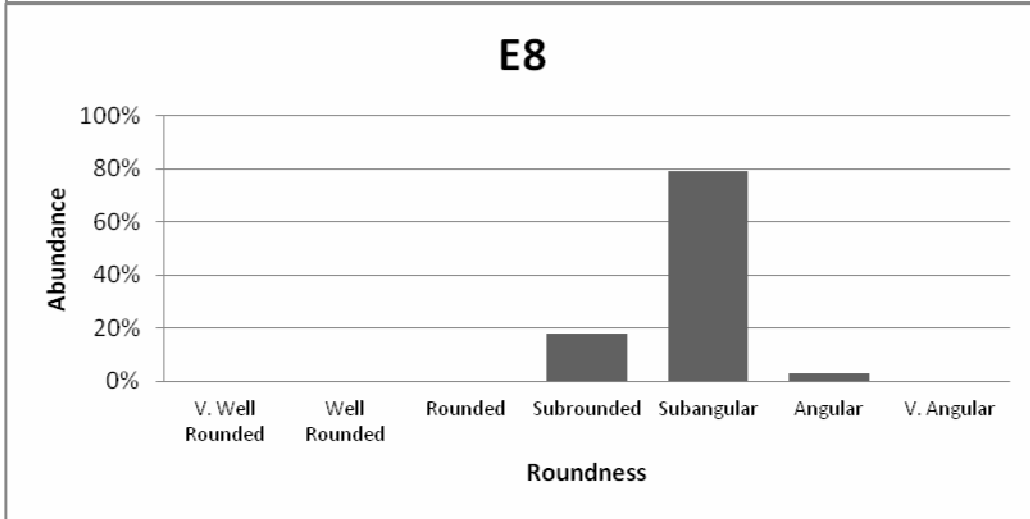
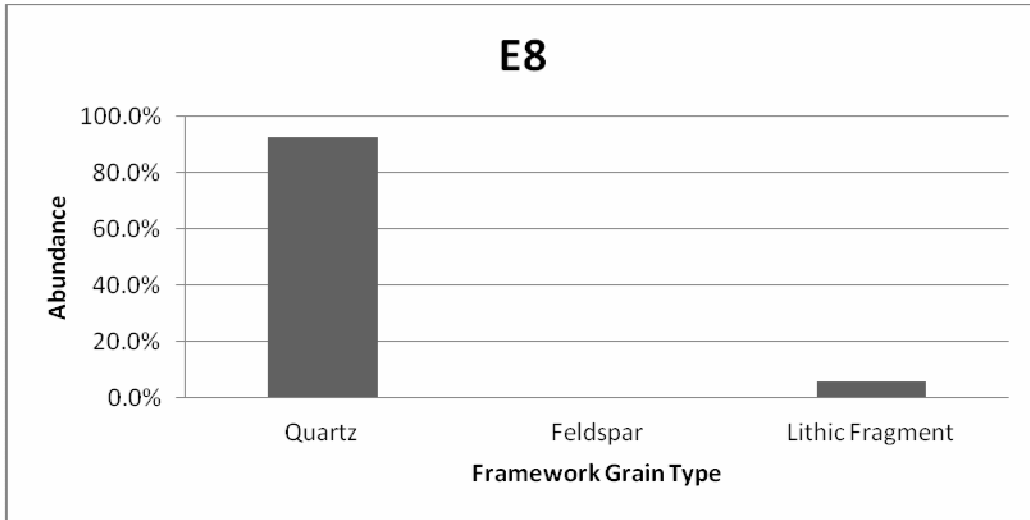
**APPENDIX A (continued)**



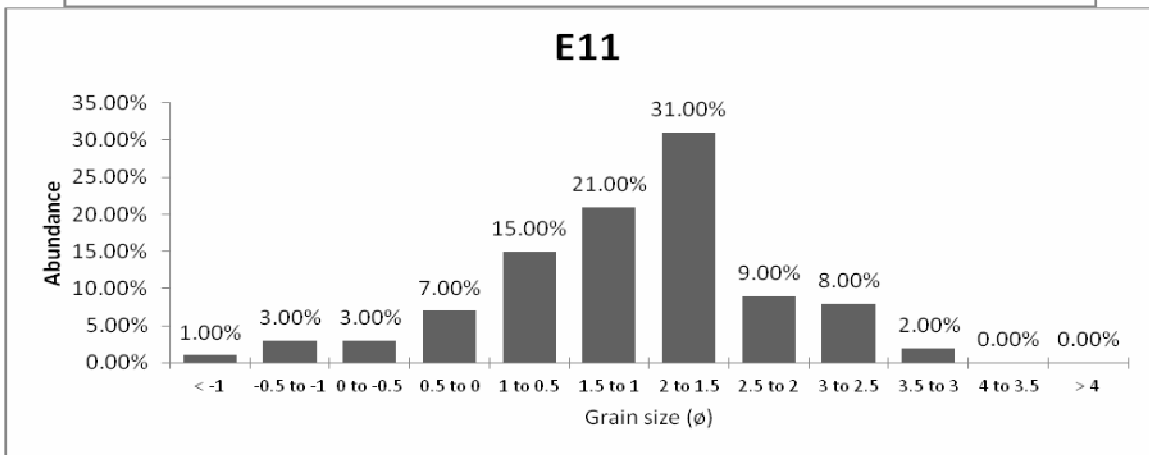
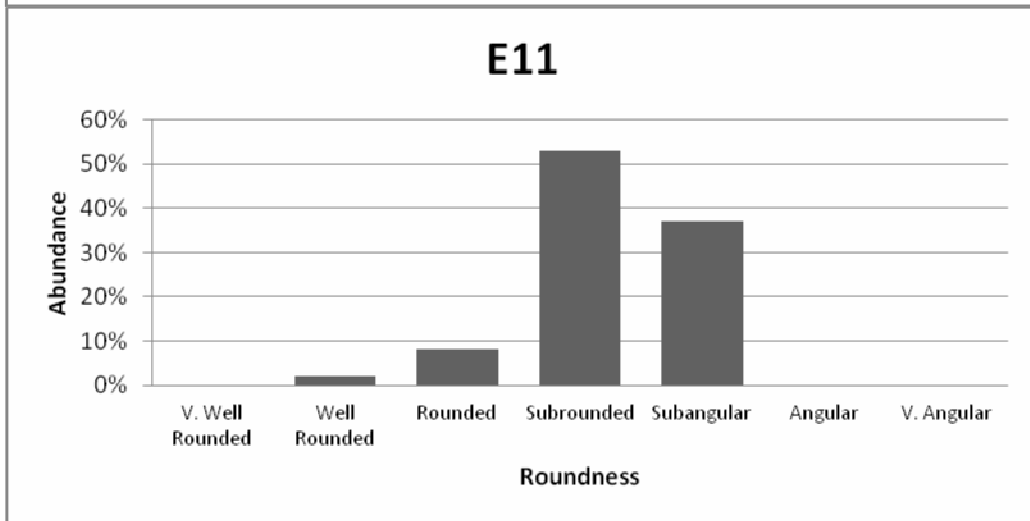
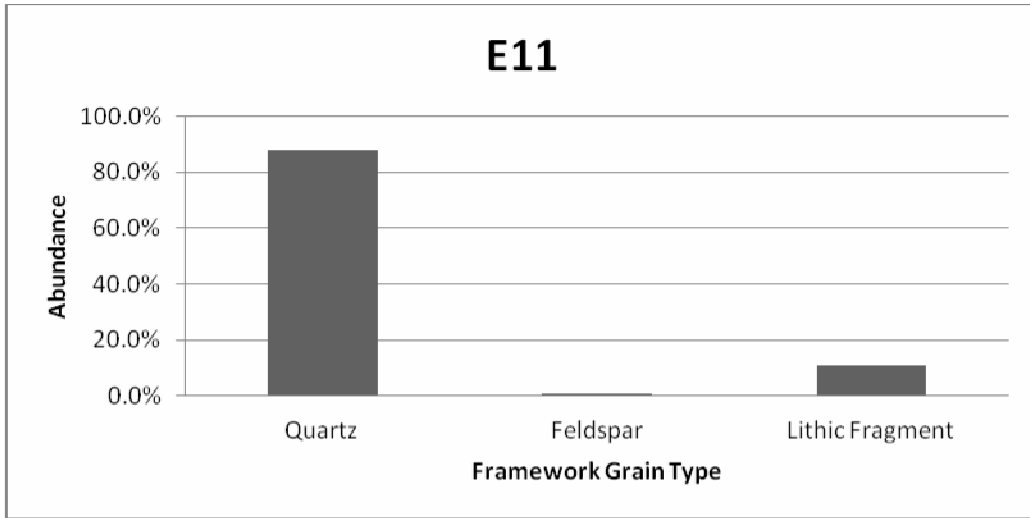
**APPENDIX A (continued)**



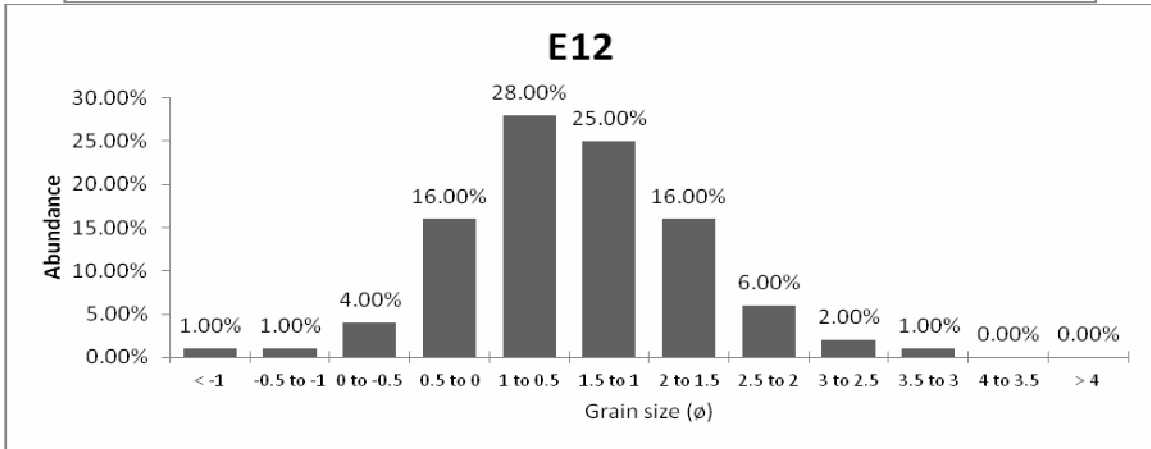
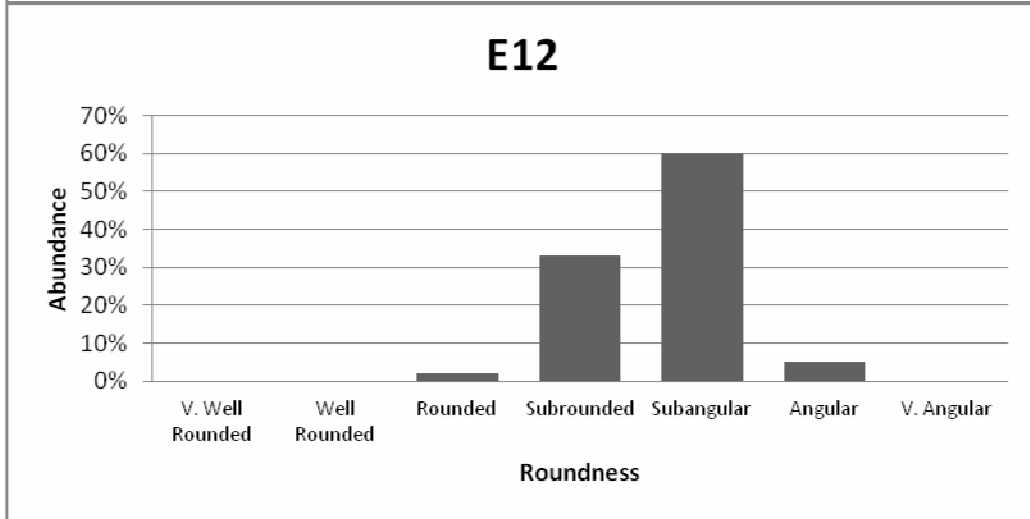
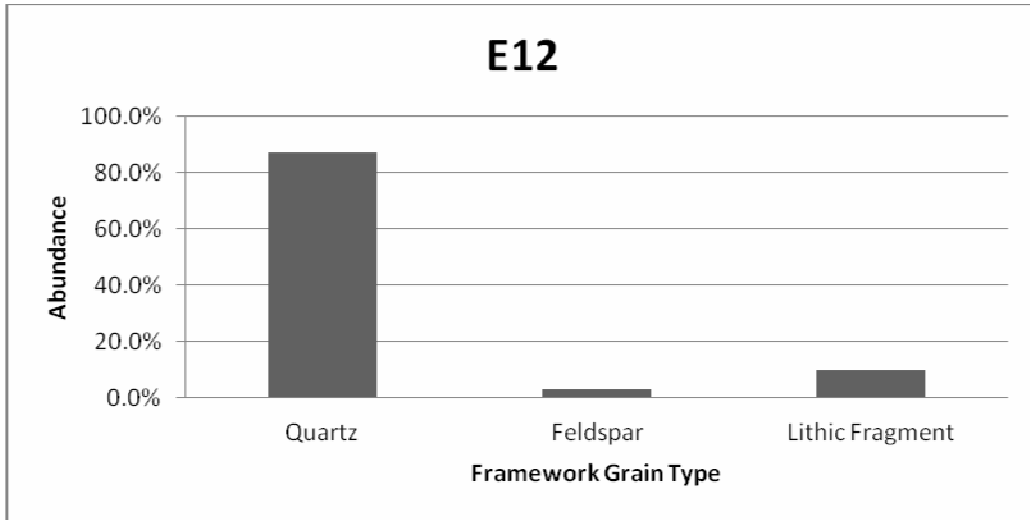
**APPENDIX A (continued)**



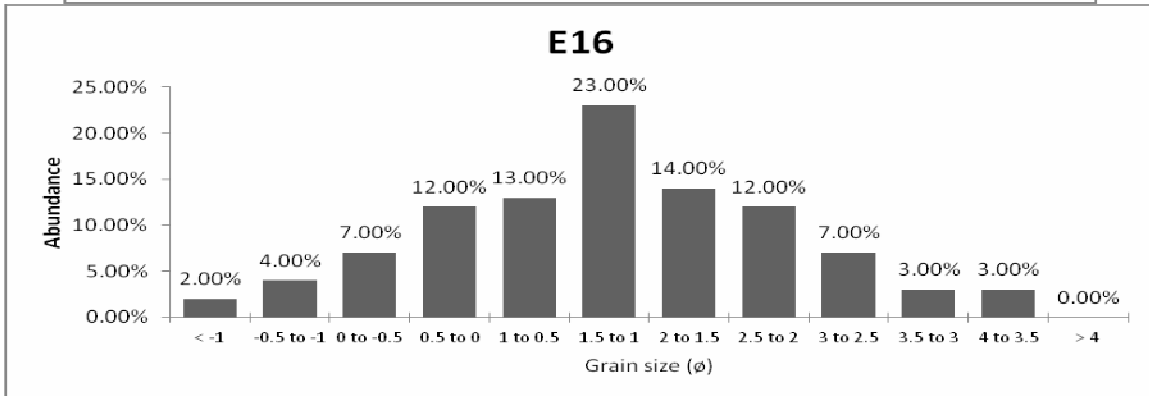
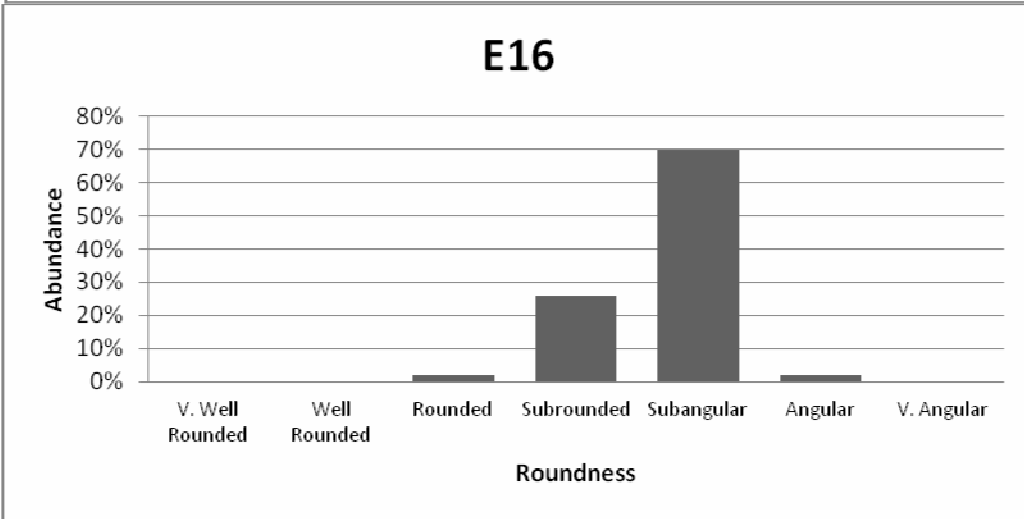
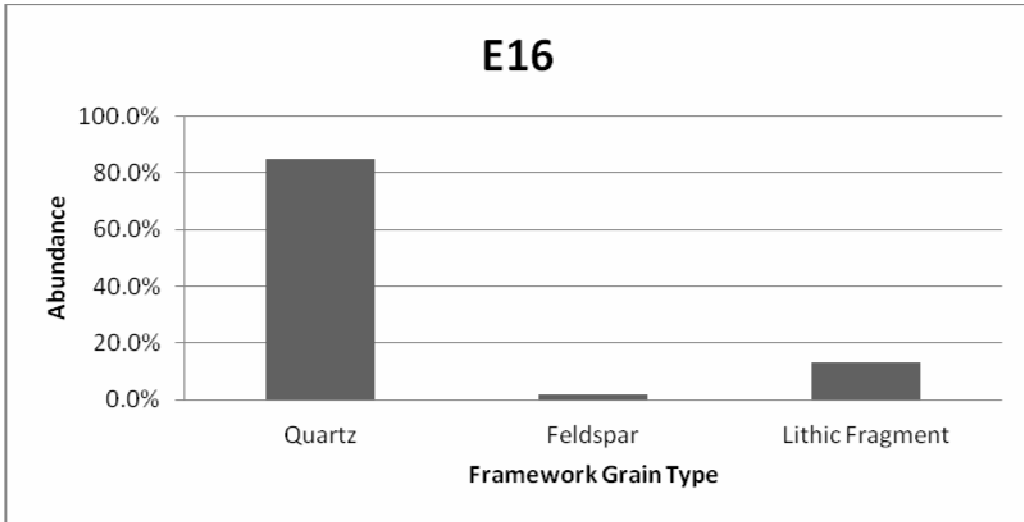
**APPENDIX A (continued)**



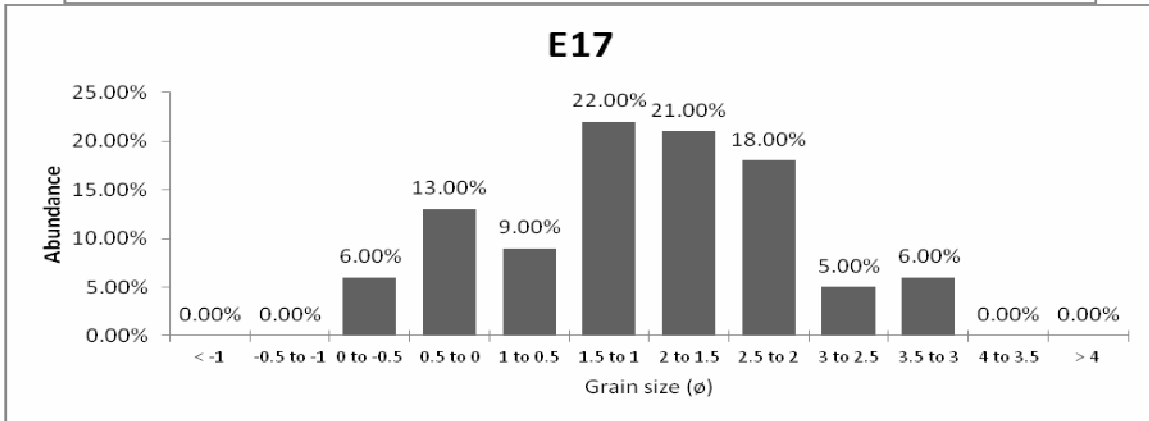
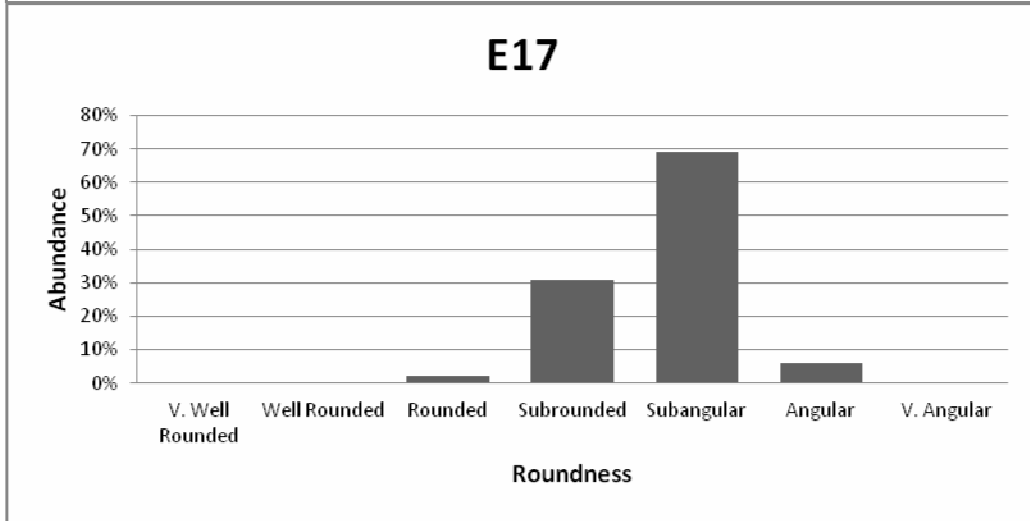
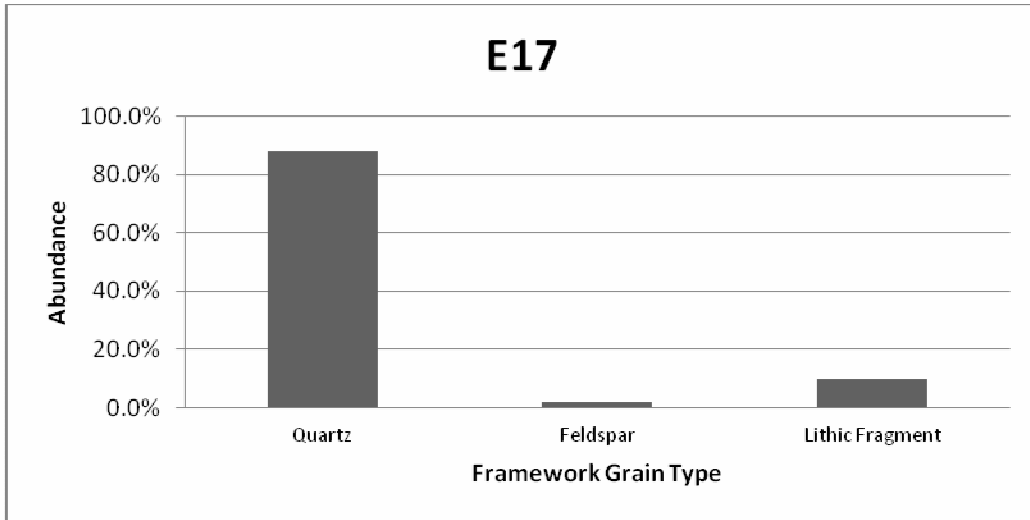
**APPENDIX A (continued)**



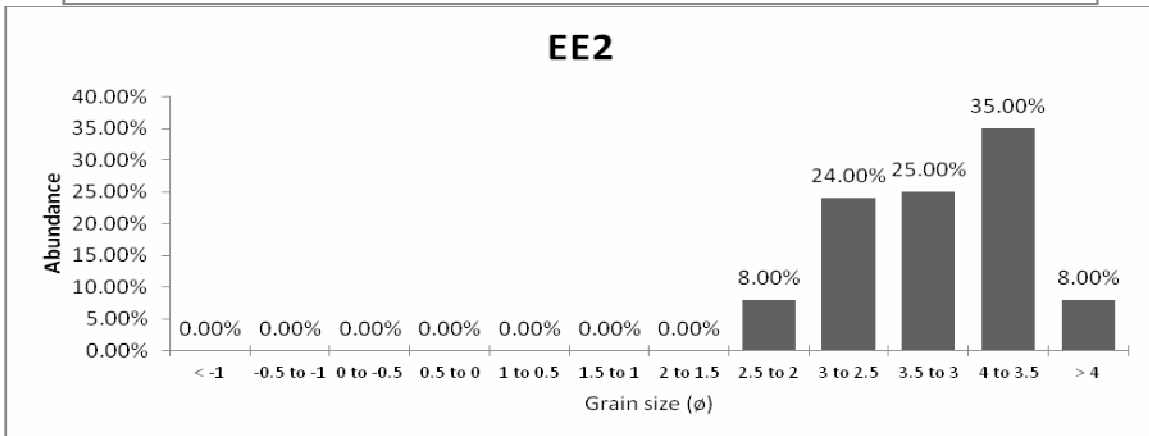
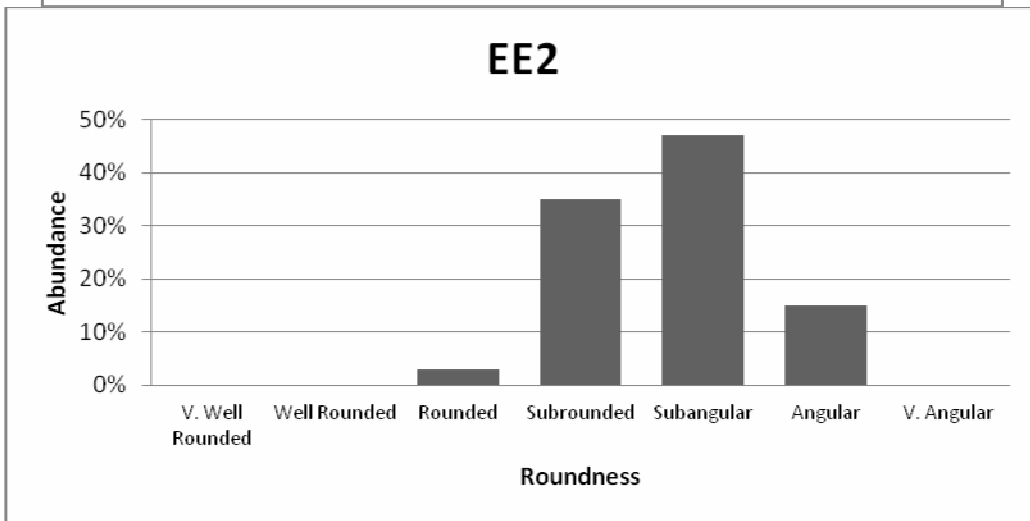
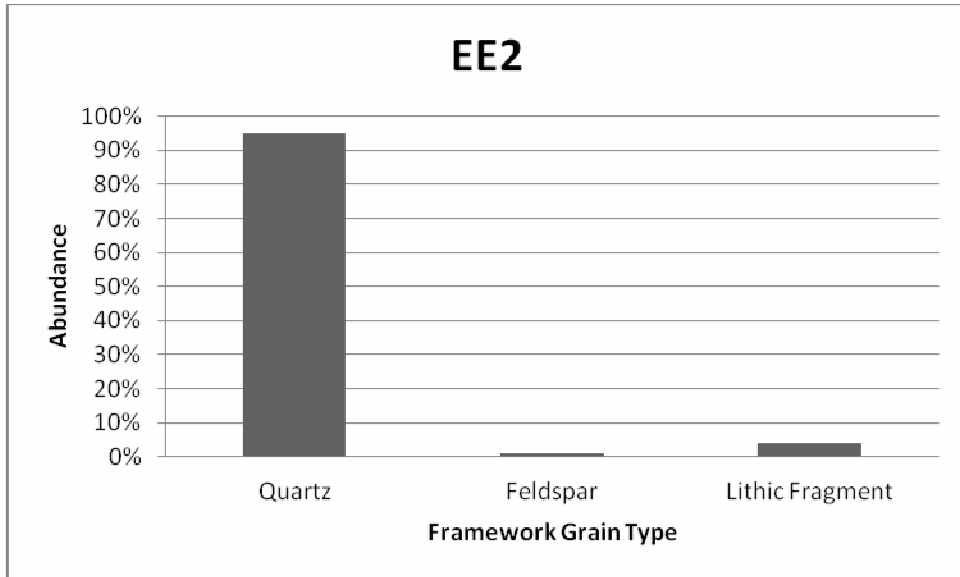
**APPENDIX A (continued)**



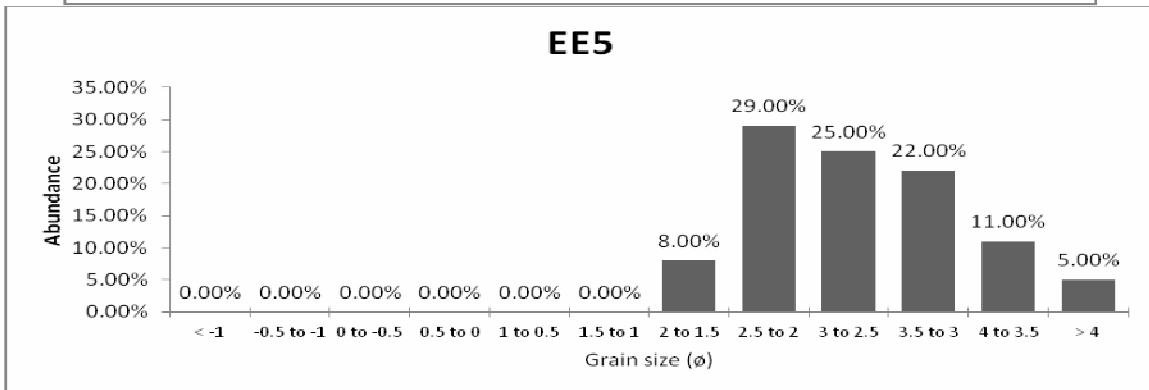
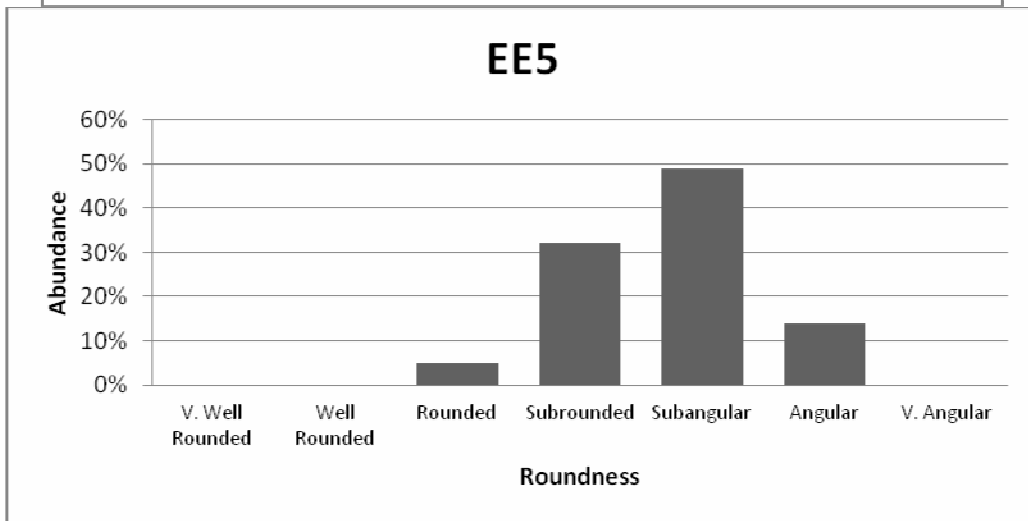
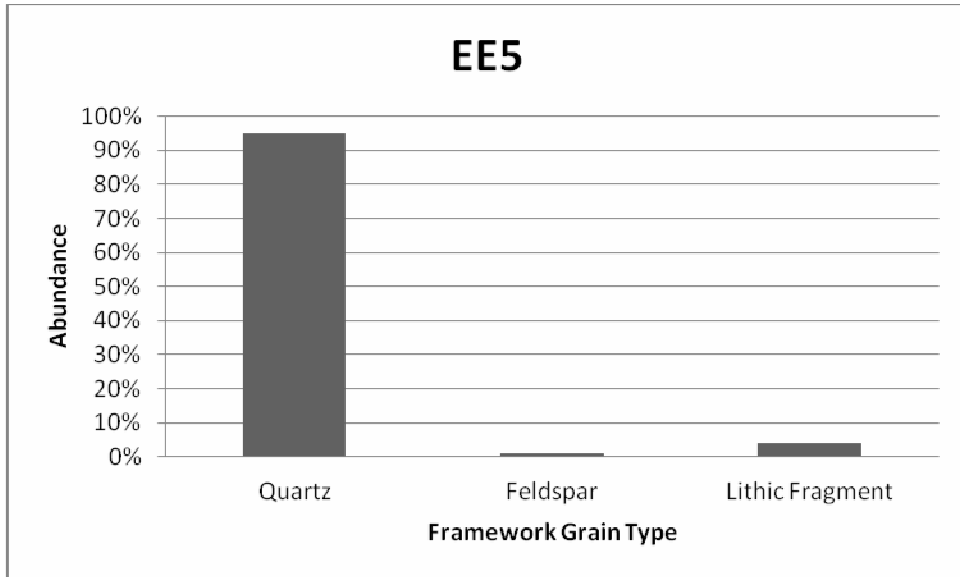
**APPENDIX A (continued)**



**APPENDIX A (continued)**



**APPENDIX A (continued)**



### APPENDIX A (continued)

W1		
Statistics		Description
Mean Grain Size ( $\phi$ )	3.28	V. fine sand
Standard Deviation ( $\phi$ )	0.59	Moderately well sorted
Skewness	0.07	Near symmetrical
Porosity (%)	7.00%	
Matrix (%)	19.00%	

W2		
Statistics		Description
Mean Grain Size ( $\phi$ )	0.91	Coarse sand
Standard Deviation ( $\phi$ )	0.85	Moderately sorted
Skewness	0.15	Fine skewed
Porosity (%)	17.20%	
Matrix (%)	3.00%	

W4		
Statistics		Description
Mean Grain Size ( $\phi$ )	1.72	Medium sand
Standard Deviation ( $\phi$ )	0.61	Moderately well sorted
Skewness	0.08	Near symmetrical
Porosity (%)	14.70%	
Matrix (%)	2.00%	

E1		
Statistics		Description
Mean Grain Size ( $\phi$ )	1.29	Medium sand
Standard Deviation ( $\phi$ )	0.81	Moderately sorted
Skewness	-0.01	Near symmetrical
Porosity (%)	15.3%	
Matrix (%)	4.0%	

E2		
Statistics		Description
Mean Grain Size ( $\phi$ )	1.96	Medium sand
Standard Deviation ( $\phi$ )	0.62	Moderately well sorted
Skewness	-0.06	Near symmetrical
Porosity (%)	15.0%	
Matrix (%)	4.0%	

### APPENDIX A (continued)

E3		
Statistics		Description
Mean Grain Size ( $\phi$ )	0.78	Coarse sand
Standard Deviation ( $\phi$ )	0.88	Moderately sorted
Skewness	0.17	Fine skewed
Porosity (%)	12.0%	
Matrix (%)	5.0%	

E6		
Statistics		Description
Mean Grain Size ( $\phi$ )	1.67	Medium sand
Standard Deviation ( $\phi$ )	0.55	Moderately well sorted
Skewness	-0.04	Nearly symmetrical
Porosity (%)	15.0%	
Matrix (%)	2.0%	

E7		
Statistics		Description
Mean Grain Size ( $\phi$ )	1.55	Medium sand
Standard Deviation ( $\phi$ )	0.75	Moderately sorted
Skewness	-0.30	Coarse skewed
Porosity (%)	15.7%	
Matrix (%)	2.0%	

E8		
Statistics		Description
Mean Grain Size ( $\phi$ )	1.75	Medium sand
Standard Deviation ( $\phi$ )	0.63	Moderately well sorted
Skewness	-0.03	Near symmetrical
Porosity (%)	15.5%	
Matrix (%)	1.0%	

E11		
Statistics		Description
Mean Grain Size ( $\phi$ )	1.42	Medium sand
Standard Deviation ( $\phi$ )	0.86	Moderately sorted
Skewness	-0.18	Coarse skewed
Porosity (%)	13.0%	
Matrix (%)	5.0%	

**APPENDIX A (continued)**

E12		
Statistics		Description
Mean Grain Size ( $\phi$ )	1.03	Medium sand
Standard Deviation ( $\phi$ )	0.75	Moderately sorted
Skewness	0.07	Near symmetrical
Porosity (%)	12.8%	
Matrix (%)	4.0%	

E16		
Statistics		Description
Mean Grain Size ( $\phi$ )	1.43	Medium sand
Standard Deviation ( $\phi$ )	1.01	Poorly sorted
Skewness	0.15	Fine skewed
Porosity (%)	9.0%	
Matrix (%)	11.0%	

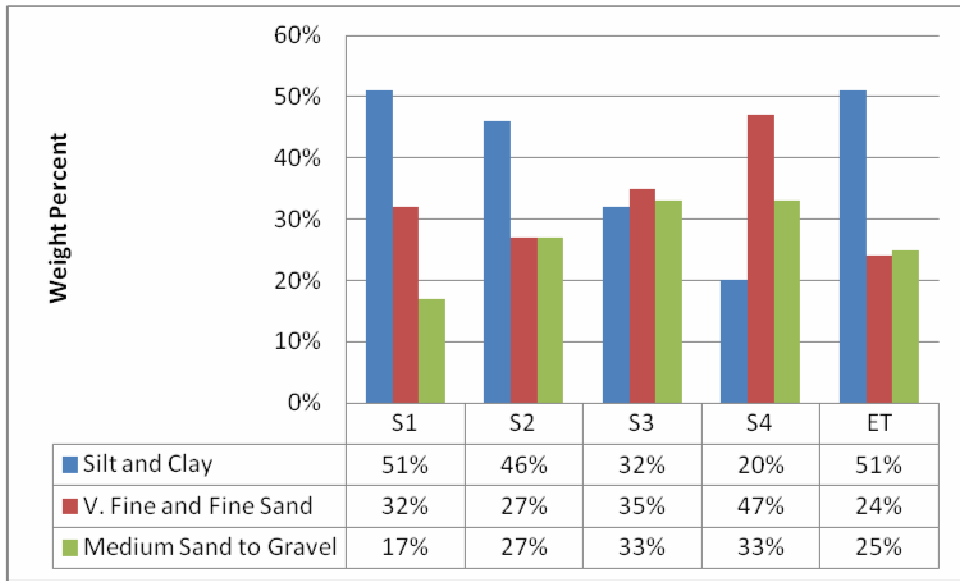
E17		
Statistics		Description
Mean Grain Size ( $\phi$ )	1.40	Medium sand
Standard Deviation ( $\phi$ )	0.98	Moderately sorted
Skewness	-0.08	Near symmetrical
Porosity (%)	8.5%	
Matrix (%)	9.0%	

EE2		
Statistics		Description
Mean Grain Size ( $\phi$ )	2.78	Fine sand
Standard Deviation ( $\phi$ )	0.83	Moderately sorted
Skewness	0.01	Near symmetrical
Porosity (%)	8.00%	
Matrix (%)	1.00%	

EE5		
Statistics		Description
Mean Grain Size ( $\phi$ )	2.25	Fine sand
Standard Deviation ( $\phi$ )	0.76	Moderately sorted
Skewness	0.09	Near symmetrical
Porosity (%)	8.00%	
Matrix (%)	1.00%	

## APPENDIX B

### SLACKWATER GRAIN-SIZE



## APPENDIX C

### MEASURED POROSITY AND PERMEABILITY

SAMPLE NO.	DEPTH ft	GRAIN DENSITY	POROSITY %	PERMEABILITY mD (PROBE)	
1	E1	2.66	15.3	466.54	PROBE
2	E7	2.65	15.7	589.22	PROBE
3	E11	2.65	13.0	80.37	PROBE
4	E12	2.65	12.8	32.28	PROBE
5	E17	2.66	8.5	12.76	PROBE
6	W2	2.64	17.2	569.20	PROBE
7	W4	2.65	14.7	206.55	PROBE

